

NOTICE:

The copyright law of the United States (Title 17, United States Code) governs the making of reproductions of copyrighted material. One specified condition is that the reproduction is not to be "used for any purpose other than private study, scholarship, or research." If a user makes a request for, or later uses a reproduction for purposes in excess of "fair use," that user may be liable for copyright infringement.

RESTRICTIONS:

This student work may be read, quoted from, cited, and reproduced for purposes of research. It may not be published in full except by permission by the author.

Albright College Gingrich Library

The Correlation of Solubility and Pi Star

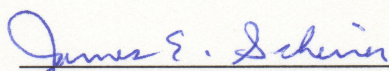
Kelly-Ann S. Bieber

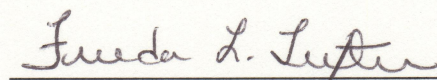
Candidate for the degree


Bachelor of Science

Submitted in partial fulfilment of the requirements for

Departmental Distinction in Chemistry & Biochemistry


James E. Scheirer, Ph.D.


Frieda L. Texter, Ph.D.


Devon B. Mason, Ph.D.

Albright College Gingrich Library

F. Wilbur Gingrich Library
Special Collections Department
Albright College

Release of Senior Honors Thesis

I hereby deliver, give, and transfer property, rights, interest in and legal rights thereto which I had, have, or may have concerning the Senior Honors Thesis described below to the Special Collections Department of the F. Wilbur Gingrich Library at Albright College as an unrestricted gift. While copyright privileges will remain with me, the author, all privileges to reproduce, disseminate, or otherwise preserve the Senior Honors Thesis are given to the Special Collections Department of the Gingrich Library. I place no restrictions on this gift and hereby indicate this by signing below.

Title: The Correlation of Solubility and Pi Star

Signature of Author: Kelly-Ann S. Bieber Date: 5/10/04

Printed Name of Author: Kelly-Ann S. Bieber

Street Address: 72 Mtn. Spring Rd. P.O. Box 352

City, State, Zip Code: Blandon, PA 19510

Albright College Gingrich Library

The Correlation of Solubility and Pi Star

Kelly-Ann S. Bieber

Albright College 2003-2004

Advisor: Dr. Scheirer

Readers: Dr. Texter and Dr. Mason

Albright College Gingrich Library

Abstract:

The ultra-violet visible spectrophotometer was used to measure the λ_{max} of a series of non-hydrogen bonding solvents. From λ_{max} , the solvent's π^* value was calculated using an equation derived by Kamlet and coworkers. Solubility studies were completed on three solutes of varying polarity using a gravimetric method. Linear regression lines were fitted to plots of π^* versus the log of solubility. Only a fair linear trend was observed; therefore, it was concluded that another factor was involved. The extent of solvent halogenation was investigated, but there was no distinct trend relating π^* to the extent of halogenation in a solvent.

Albright College Gingrich Library

Introduction:

In previous years, research studies have been conducted to explore the correlation of π^* with various experimental parameters such as thermodynamic and kinetic properties. However, a limited number of studies have attempted to find a direct correlation between the π^* and solubility. In 1977 Kamlet, Abboud, and Taft published a π^* scale that related the shift in the ultraviolet-visible absorbance maximum wavelength for a particular dye in a solvent to solution properties. According to Kamlet, et al, π^* is a measurement of solvent polarity-polarizability since the shift results from the solvent's affects on the $p \rightarrow \pi^*$ and $\pi \rightarrow \pi^*$ electronic transitions of the dye¹. This shift to longer wavelength and lowered energy gap is classified as a bathochromic or red shift. The greater the bathochromic shift, the greater the polarity-polarizability of the solvent. Through this research, Kamlet and coworkers¹ were able to establish the equation below relating π^* and various solvent parameters.

$$XYZ = XYZ_0 + s\pi^* + a\alpha + b\beta \quad \text{Eq. (1)}$$

where XYZ is some property, in this case solubility, XYZ_0 is the numerical value of the reference solvent's property, $a\alpha$ and $b\beta$ are terms that introduce the effects of hydrogen bonding, and s is the susceptibility of the XYZ term to the solvent's π^* values. Terms $a\alpha$ and $b\beta$ are eliminated from the equation by utilizing only those solvents that do not participate in hydrogen bonding interactions. By removing those terms the equation is reduced to the following

$$XYZ = XYZ_0 + s\pi^* \quad \text{Eq. (2)}$$

because the hydrogen bonding interactions are essentially zero. The property of π^* is determined numerically by the following equation when a single probe dye is used.

$$\pi^* = (\bar{\nu}_{\max} - \bar{\nu}_0)/s \quad \text{Eq. (3)}$$

where ν_0 is the wavenumber of the peak maximum for the reference solvent cyclohexane, ν_{\max} is the value for the solvent whose π^* is being determined, and s is defined by equation 4.

$$s = \bar{\nu}_{\text{cyclohexane}} - \bar{\nu}_{\text{DMSO}} \quad \text{Eq. (4)}$$

Cyclohexane and DMSO are used as reference solvents in this study. Cyclohexane, a nonpolar compound, is assigned a π^* of zero, and DMSO, a polar compound, is assigned a π^* of 1.

Initially Kamlet's π^* scale and equation was based upon seven indicator dyes and 28 solvent π^* values, but was later expanded to seventy-two π^* values. In 1979, Kamlet, Hall, Boykin, and Taft² examined the use of nine solvatochromic indicators in order to determine the π^* values of an additional 23 solvents. Once these π^* values were determined and the π^* scale was expanded, Kamlet, et al used the π^* values to rationalize solvent effects on rates of the Menschutkin reaction, rates of a peroxyester thermal decomposition, and free energies of transfer of a tetraalkylammonium halide between solvents². Kamlet, et al found that all three of these properties could be accurately correlated using the polarity-polarizability scale, based on electronic spectra².

Kamlet and Abboud have performed numerous studies since 1979 that have investigated other parameters affecting solvent interactions in hopes of finding an equation that most accurately characterizes π^* ³. They have also implemented studies utilizing different probe molecules in order to determine which probe solute provides the most accurate results⁴.

The Kamlet and Abboud study is applicable to the solvation of solutes in supercritical fluids as researched by Abbott and coworkers^{5,6,7,8,9}. Supercritical fluids are becoming commonly used as a media for extractions because of the marked changes in solute properties with respect to temperature and pressure changes. Abbott and coworkers⁷ studied the solubility of salicylic acid in HFC 134a in carbon dioxide with respect to its solubility in carbon dioxide alone. They found that adding a modifying solvent such as HFC 134a increases the solvent polarity and therefore increases the solute solubility. In supercritical fluids, changing pressure modifies the π^* values which are monitored as a function of pressure more easily than taking direct measurements of solubility in supercritical fluids.

In 1999, A.P. Abbott, et al⁵, performed preliminary work on the solubility and solvent properties of supercritical fluids using a high-pressure capacitative cell. Abbott and coworkers^{6,7,8} performed multiple studies using a variety of supercritical fluids including 1,1,1,2- tetrafluoroethane, difluoromethane, and pentafluoroethane. In a recent and continuing study, Abbott, et al⁹, studied the solubility of a series of substituted aromatic hydrocarbons in difluoromethane (HFC 32) in comparison with their solubility in supercritical CO₂ (scCO₂). Once again the work used a capacitative method to collect solubility data, which proved to be of limited use for scCO₂, but was effective for HFC 32. This study demonstrated that the solubility of a particular solute is dependent on pressure, polarity, and the relative positioning of substituent groups.

Research into the correlation of π^* and solubility was most recently investigated in 2001 by Bryan Platt for his senior honors project. Platt found that 4-nitroanisole served as a good probe for the investigation of λ_{max} , because of its high

extinction coefficient. Its high extinction coefficient allows measurements to be taken at a low concentration, therefore minimizing solute-solute interactions and permitting the spectra to represent only solute-solvent interactions¹⁰. Using 4-nitroanisole as a probe, Platt was able to calculate π^* for a variety of non-hydrogen bonding solvents. In a solubility study, he investigated the polar compound, salicylic acid. He found that a plot relating solubility of salicylic acid in mol/L to π^* produced an exponential curve, and a linear relationship was found when relating the log of solubility measurements to π^* . The second correlation produced a fair fit and showed that there was a direct correlation between solubility and π^* ; however, additional research would be necessary to maximize the predictability of the relationship.

The purpose of this research was to maximize the predictability of the relationship between π^* and solubility as established by Bryan Platt. To study solubility, three solutes p-chlorobenzoic acid, p-amino phenol, and p-toluic acid were selected based on their polarity and structure. Solubility studies were completed by Abbott and coworkers⁹ on these three solutes using supercritical HFC32 as a solvent at 363K. They found the solubility of p-aminophenol to increase at increasing pressures. The solubilities of p-chlorobenzoic acid and p-toluic were found to increase with increasing pressure as well. p-Chlorobenzoic acid was found to be less soluble in HFC32 at 363K than p-toluic acid.

Experimental:

Solubility studies were completed by dissolving each of the solutes listed in Table I in each of the solvents listed in Table II (except DMSO) to prepare saturated solutions. After standing one week, the saturated solutions were gravity filtered, and a 10mL aliquot was pipetted into a tared weighing bottle. The solvent was allowed to

evaporate and the bottles were reweighed after one week. From this mass, the solubility was determined in mol/L. Duplicate tests were obtained for each saturated solution.

π^* values were determined by dissolving a minimal amount of 4-nitroanisole in a 1cm quartz cuvette. The UV-visible spectrophotometer was used to obtain the UV-vis spectrum of each solvent over the range of 350-250nm, using the pure solvent in the reference beam. After the initial scan, multiple scans were taken over a smaller wavelength range in order to focus in on the maximum absorbance wavelength. A minimum of ten scans were obtained and averaged for each solvent. Because of variation in π^* values, a second series of UV-vis scans were obtained for some solvents and were averaged with the first series.

Results:

The ultraviolet visible scans for each solvent over the range of 350-250 nm are shown in Figures 1 through 22. Duplicate scans indicate solvents whose series were rescanned. Multiple scans were recorded for each solvent, and the maximum absorbance wavelengths, the average of the scans, and 95% confidence interval are shown in Table III. By converting the average maximum absorbance wavelengths of cyclohexane and DMSO to wavenumbers and using equation 4 above, the constant s was determined to be -2504.25cm^{-1} . Next, using equation 3 and the average maximum absorbance wavelength of each solvent, π^* was determined for each solvent. π^* values are shown in Table IV.

Solubility data was calculated for each solute and is shown in Table V through VII. The masses are listed as A and B in the corresponding table. Molar solubility was calculated by dividing by the molecular weight of the solute and dividing by the volume

of the aliquot, .010 L. The average solubility and the log of average solubility were calculated.

Figure 23 shows the plot of pi star verses the log of molar solubility of p-chlorobenzoic acid. The equation of a linear least squares fit is $y = .5968x - 2.7022$ with an r^2 value of .6216. Figure 24 shows the plot of pi star verses the log of molar solubility of p-aminophenol. The equation of a linear least squares fit is $y = .5637x - 2.8335$ with an r^2 value of .1125. Figure 25 shows the plot of pi star verses the log of molar solubility of toluic acid. The equation of the linear least squares fit is $y = 1.0544x - 1.681$ with an r^2 value of .6982. Each plot was fit with linear regression lines based on the correlation established by Platt in 2001.

Figure 26 shows pi star verses log of molar solubility for all three test solutes. This plot places all the test solutes on the same scale and a relationship can be developed between the three solutes. Toluic acid is observed to be the most soluble and p-aminophenol is observed to be the least soluble.

Discussion:

As shown in Figures 1 through 22, the ultraviolet-visible spectra obtained for the series of solvents used in this experiment did not yield an extremely smooth, distinct peak. Use of the UV-vis software package allowed curve smoothing to be completed, so that a more accurate value of maximum absorbance wavelength could be determined. Using this smoothing technique, λ_{\max} could be reproduced on a fairly consistent basis. The average of a series of at least ten scans provided results with minimal 95% confidence intervals. Most maximum wavelengths were established within a confidence

interval of .25-.75. This margin for error is relatively small in comparison to the actually values obtained for wavelength.

Upon conversion of these wavelengths to pi star values, it was observed that many of the pi star values obtained in this experiment yielded results similar to those results obtained by Platt in 2001. Another researcher, Robert Luo, who is also completing pi star studies, obtained pi star values consistent with those obtained in this experiment. Pi star values appear to be fairly reproducible for most solvents. Some solvents needed additional study, and were found to produce slightly different pi star values when they were remeasured. As mentioned above these multiple values were averaged with the originals.

The solubility portion of this research was the most reproducible part of this experiment. As stated above, duplicate solubility tests were run for each saturated solution. These duplicate tests produced precise results within approximately .0001-.0005g. Even though the gravimetric procedure for determination of solubility may appear elementary in concept, it proved to be a reproducible and valuable technique for this research.

Three solutes, p-chlorobenzoic acid, p-aminophenol, and p-toluic acid, were examined in the solubility portion of the experiment. All three solutes were polar compounds, and were expected to be fairly soluble because of their polar nature. As predicted in the work of Abbot and coworkers, p-aminophenol was less soluble than p-chlorobenzoic acid, which was less soluble than p-toluic acid. This relationship could also be predicted based on the structure of these compounds alone. Toluic acid contains a carboxyl functionality para to a methyl group on a benzoic acid. This carboxyl group

creates a dipole, which makes the solute more soluble in the series of solvents used. In comparison, p-chlorobenzoic acid contains a carboxyl group para to a chlorine atom on a benzene ring. Since these polar groups are opposite to each other on the ring, the net polar effect is weakened therefore decreasing the solubility in the solvent. Lastly, p-aminophenol is the least soluble because it contains functional groups of less polarity.

Polarity was not the only factor in determining solubility of a solute. Both p-chlorobenzoic acid and p-toluic acid produced solubility results that were both accurate and precise; however, p-aminophenol produced results that were precise but not accurate. Upon preparation and standing of saturated solutions of p-aminophenol, the solute produced a black or brown colored precipitate, or the solvent's color changed to a clear yellow solution. Investigation of the properties of p-aminophenol lead to the conclusion that p-aminophenol undergoes an oxidization reaction in some solvents.

Taking the data obtained for the UV-vis spectrophotometer and the solubility study, a correlation was established between pi star and solubility. Platt's study in 2001 indicated that a fair linear fit was established between the two properties; therefore, that is the direction this researcher followed. Figure 23 shows the correlation established between pi star and the log of the solubility of p-chlorobenzoic acid. As pi star increases the log of solubility is observed to increase, therefore producing a fair linear trend with a correlation coefficient of .6216.

Figure 24 shows the correlation established between pi star and the log of solubility of p-aminophenol. As stated above, the solubility study for this solute was flawed and that is why such a weak correlation of .1125 was established between pi star

and solubility. One could conclude that studies utilizing solutes with hydroxyl functionalities must be completed in non-oxidizing systems.

Figure 25 shows the correlation established between π star and the log of the solubility of p-toluic acid. Again, as π star increases, the log of solubility also increases. There is a slightly stronger correlation coefficient of .6982 for this data series, which may be attributable to the fact that p-toluic acid is a more polar compound than p-chlorobenzoic acid and p-aminophenol.

Figure 26 shows all three correlations and the results of Platt's research on the solubility of salicylic acid on the same scale. Ignoring p-aminophenol, because of inaccurate solubility data, the trends observed for p-toluic acid and p-chlorobenzoic acid are similar. The tighter correlation for the data points for p-toluic acid are most likely a result of its increased polarity. In comparison to Platt's results, the correlation developed in this research is weaker. Platt's research produced π star values that spanned the π star scale instead of clustering at the center as my results did. This clustering weakened my data series, and therefore weakened my correlation.

Although a linear fit is established between π star and log of solubility, the correlation is not as strong as this researcher and others would have predicted. One problem encountered in this research is that many solvents yielded π star values in the range .380 to .450. This collection of data points at the center of the scale left minimal data points for the extremes of the scale. Another possible research target for the future could include examination of a solvent's structure as a prediction of π star. Having this knowledge would have made finding solvents with certain π star values easier.

The predictability of the relationship between π star and solubility was not established as well as I expected in this research. There may be another factor involved, which is not taken into account in this study. From Figures 23-26, it is observed that solubility does increase with increasing π star values and a fair linear trend is observed, but the correlation is weak.

In an attempt to identify the other factor effecting the correlation between π star and solubility, I examined the effect of non-halogenated, mono-halogenated, and poly-halogenated solvents. The plot shown in Figure 27 was constructed for the p-chlorobenzoic acid. A linear regression line was fitted to each solvent type data series. This study did not include many non-halogenated solvents, therefore with only two data points a correlation could not accurately be established for those solvents. The mono-halogenated and the poly-halogenated solvents were fitted with a linear trend line. They did not show a good linear fit. There is a lot of scatter observed in this correlation, therefore leading me to believe that the extent of halogenation is not the effect limiting the correlation of π star and solubility.

In conclusion, the correlation between π star and solubility must be affected by a factor that was not taken into consideration in this study. Further research may maximize that predictability of the relationship between π star and solubility; however at this point only a far linear relationship is established using solutes of varying polarity.

Glossary

Bathochromic shift or red shift – characterized by a shift in λ_{max} to a longer wavelength in the ultra-violet visible spectrum with a decrease in the energy gap

Lambda maximum - λ_{max} – the ultra-violet visible wavelength in nanometers at maximum absorbance

Pi star - π^* - the polarity-polarizability of a solvent

Supercritical fluid – a substance above its critical temperature and critical pressure.

Critical temperature and pressure are defined as the limits at which a substance exists in liquid-vapor equilibrium.

Albright College Gingrich Library

References

1. Kamlet, M.J., J.L. Abboud, and R.W. Taft. "The Solvatochromic Comparison Method. 6. The π^* Scale of Solvent Polarities." J. Am. Chem. 99 (1977): 6027-6038.
2. Kamlet, M.J., T.N. Hall, J. Boykin, and R.W. Taft. "Linear Solvation Energy Relationships. 6. Additions to and Correlations with the π^* Scale of Solvent Polarities." J. Organic Chem. 44 (1979): 2598-2604.
3. Kamlet, M.J., J.L. Abboud, M.H. Abraham, R.W. Taft. "Linear Solvation Energy Relationships. 23. A Comprehensive Collection of the Solvatochromic Parameters, π^* , α , and β , and Some Methods for Simplifying the Generalized Solvatochromic Equation." J. Org. Chem. 48 (1983): 2877-2887.
4. Abboud, J.L., C. Laurence. "Empirical Treatment of Solvent-Solute Interactions." J. Phys. Chem. 98 (1994): 5808-5817.
5. Abbott, A.P., C.A. Eardley, and R. Tooth. "Relative Permittivity Measurements of 1,1,1,2-Tetrafluoroethane (HFC 134a), Pentafluoroethane (HFC 125), and Difluoromethane (HFC 32)." J. Chem. Eng. Data. 44 (1999): 112-115.
6. Abbott, A.P., C.A. Eardley, and J.E. Scheirer. "Solvent Properties of Supercritical CO₂/HFC134a Mixtures." J. Phys. Chem. 103 (1999): 8790-8793.
7. Abbott, A.P., C.A. Eardley, and J.E. Scheirer. "CO₂/HFC 134a Mixtures: Alternatives for Supercritical Fluid Extraction." The Royal Society of Chemistry. Apr. (2000): 63-65.

8. Abbott, A.P., C.A. Eardley, and J.E. Scheirer. "Analysis of Dipolarity/polarisability parameter, π^* , for a Range of Supercritical Fluids." Phys. Chem. Chem. Phys. 3 (2001) 3722-3726.
9. Abbott, A.P., N.E. Durling, W. Eltringham, and E.G. Hope. "Solid Solubility Studies in Supercritical Fluids." (work in progress)
10. Platt, Bryan J, and J.E. Scheirer (advisor) "Correlation of Solubility and π^* . Senior Research Project (2001)

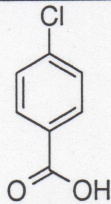
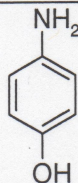
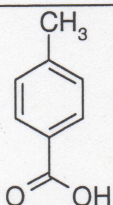
Table I: Solute Properties		
Compound	Molecular Weight	Structure
p-chlorobenzoic acid	156.67 g/mol	
p-aminophenol	109.13 g/mol	
p-toluic acid	136.15 g/mol	

Table II: Solvents
hexane
cyclohexane
carbon tetrachloride
tetrachloroethylene
1-chlorobutane
1-bromobutane
1,1,1-trichloroethane
bromoethane
trichloroethylene
2-bromobutane
2-bromopropane
1-bromopropane
1,2-dibromoethane
methylene chloride
1,1,2,2-tetrachloroethane
dibromomethane
DMSO

Albright College Gwgrich Library

Table III: UV-vis Maximum Absorbance Wavelengths

Solvent	$\lambda_{\max 1}$	$\lambda_{\max 2}$	$\lambda_{\max 3}$	$\lambda_{\max 4}$	$\lambda_{\max 5}$	$\lambda_{\max 6}$	$\lambda_{\max 7}$	$\lambda_{\max 8}$	$\lambda_{\max 9}$	$\lambda_{\max 10}$	$\lambda_{\max 11}$	$\lambda_{\max 12}$	$\lambda_{\max 13}$	$\lambda_{\max 14}$	Average	95% Confidence
2-bromobutane	301.8	303.2	302.6	303.5	304.1	302.0	303.2	303.0	303.6	303.2	303.5	301.8	303.0	304.4	303.1	0.46
2-bromopropane	301.5	304.3	303.7	302.9	301.6	304.6	304.4	301.7	302.4	304.6	304.1	303.5	303.5	302.9	303.3	0.65
1,1,2,2-tetrachloroethane	312.3	312.3	311.8	312.6	311.9	312.4	312.0	311.0	312.1	312.3	---	---	---	---	312.1	0.32
1,1,2,2-tetrachloroethane (2)	312.0	313.0	312.0	312.7	314.0	314.1	312.5	313.7	312.3	313.5	312.8	312.4	---	---	312.9	0.47
1,1,1-trichloroethane	303.3	303.6	302.5	302.5	301.8	302.5	302.5	302.7	303.0	302.8	303.8	301.9	---	---	302.7	0.39
1-chlorobutane	302.2	301.9	302.3	301.8	302.5	302.8	302.4	302.4	302.8	301.9	---	---	---	---	302.3	0.25
1-chlorobutane (2)	303.1	302.1	302.8	301.8	301.9	301.7	302.3	302.0	301.5	301.5	301.5	301.8	---	---	302.0	0.33
Cyclohexane	294.1	293.3	294.1	293.6	293.0	293.9	293.2	293.6	293.5	293.5	---	---	---	---	293.6	0.26
1-bromopropane	304.5	304.5	304.2	303.4	303.4	304.3	303.7	302.7	303.2	304.2	303.8	304.1	---	---	303.8	0.36
trichloroethylene	302.7	302.2	302.7	302.6	303.2	303.3	302.4	303.1	302.4	302.9	---	---	---	---	302.8	0.26
dibromomethane	312.6	312.4	312.9	313.5	312.7	312.3	312.3	312.7	312.7	313.4	312.9	312.5	---	---	312.7	0.25
dibromomethane (2)	312.2	313.1	314.7	312.6	312.9	314.7	311.7	313.7	314.1	312.9	---	---	---	---	313.3	0.73
Methylene Chloride	310.1	308.1	307.9	309.4	310.2	308.7	308.7	307.7	309.2	308.3	309.2	307.9	---	---	308.8	0.54
Hexanes	290.0	290.6	291.7	292.1	291.8	290.9	290.9	292.4	290.6	290.4	290.5	291.5	---	---	291.1	0.48
Tetrachloroethylene	299.8	300.0	299.5	299.6	299.2	298.9	300.0	299.3	299.2	300.2	299.1	299.7	---	---	299.5	0.26
1-bromobutane	302.1	302.4	302.6	302.5	302.5	302.5	302.8	302.3	302.3	302.7	---	---	---	---	302.5	0.15
bromoethane	302.3	302.4	302.1	302.0	302.3	304.3	302.4	302.5	303.0	302.9	302.4	303.3	303.3	303.1	302.7	0.36
bromoethane (2)	305.5	305.9	306.0	305.7	305.1	306.3	305.0	305.5	305.4	305.3	---	---	---	---	305.6	0.29
1,2-dibromoethane	309.3	307.4	307.3	308.6	308.4	307.2	307.6	308.9	308.5	308.8	308.3	309.2	---	---	308.3	0.47
1,2-dibromoethane (2)	309.5	310.0	310.8	308.6	308.7	309.7	308.7	309.2	309.7	308.3	308.6	310.2	---	---	309.3	0.49
carbon tetrachloride	297.0	298.7	296.8	298.5	297.7	298.4	297.2	297.1	298.3	297.5	298.4	296.7	297.9	296.6	297.6	0.43
DMSO	316.8	317.6	317.0	316.5	317.1	316.3	316.7	317.7	317.1	316.4	---	---	---	---	316.9	0.34

Table IV: Solvent Pi Star Values			
Solvent	Average λ_{\max}	Wavenumber	π^*
2-bromobutane	303.1	32992	0.426
dibromomethane	312.7	31980	0.831
1-bromopropane	303.8	32916	0.457
methylene chloride	308.8	32383	0.669
1-chlorobutane	302.3	33080	0.391
hexane	291.1	34352	-0.117
1,1,1-trichloroethane	302.7	33036	0.409
tetrachloroethylene	299.5	33389	0.268
trichloroethylene	302.8	33025	0.413
2-bromopropane	303.3	32971	0.435
1,1,2,2-tetrachloroethane	312.1	32041	0.806
carbon tetrachloride	297.6	33602	0.183
cyclohexane	293.6	34060	0.000
1-bromobutane	302.5	33058	0.400
bromoethane	302.7	33036	0.409
1,2-dibromoethane	308.3	32436	0.649
DMSO	316.9	31556	1.000

Table V: Solubility Data for p-chlorobenzoic acid						
Solvent	Mass A	Mass B	Solubility A	Solubility B	Average Solubility	log Solubility
2-bromobutane	0.0083	0.0082	0.00530	0.00524	0.00527	-2.278
dibromomethane	0.0064	0.0063	0.00409	0.00402	0.00406	-2.392
1-bromopropane	0.0062	0.0063	0.00396	0.00402	0.00399	-2.399
methylene chloride	0.0075	0.0076	0.00479	0.00485	0.00482	-2.317
1-chlorobutane	0.0067	0.0064	0.00428	0.00409	0.00418	-2.378
hexane	0.0034	0.0035	0.00217	0.00224	0.00220	-2.657
1,1,1-trichloroethane	0.0059	0.0057	0.00377	0.00364	0.00370	-2.431
tetrachloroethylene	0.0033	0.0033	0.00211	0.00211	0.00211	-2.676
trichloroethylene	0.0069	0.0067	0.00441	0.00428	0.00434	-2.362
2-bromopropane	0.0045	0.0046	0.00287	0.00294	0.00291	-2.537
1,1,2,2-tetrachloroethane	0.0093	0.0092	0.00594	0.00588	0.00591	-2.229
carbon tetrachloride	0.0033	0.0031	0.00211	0.00198	0.00204	-2.690
cyclohexane	0.0018	0.0018	0.00115	0.00115	0.00115	-2.939
1-bromobutane	0.0065	0.0064	0.00415	0.00409	0.00412	-2.385
bromoethane	0.0077	0.0071	0.00492	0.00453	0.00473	-2.325
1,2-dibromoethane	0.0082	0.0081	0.00524	0.00517	0.00521	-2.284
DMSO	---	---	---	---	---	---

Table VI: Solubility Data for p-aminophenol						
Solvent	Mass A	Mass B	Solubility A	Solubility B	Average Solubility	log Solubility
2-bromobutane	0.0055	0.0050	0.00504	0.00458	0.00481	-2.318
dibromomethane	0.0052	0.0052	0.00476	0.00476	0.00476	-2.322
1-bromopropane	0.0025	0.0028	0.00229	0.00257	0.00243	-2.615
methylene chloride	0.0031	0.0038	0.00284	0.00348	0.00316	-2.500
1-chlorobutane	0.0008	0.0006	0.00073	0.00055	0.00064	-3.193
hexane	0.0045	0.0051	0.00412	0.00467	0.00440	-2.357
1,1,1-trichloroethane	0.0012	0.0011	0.00110	0.00101	0.00105	-2.977
tetrachloroethylene	0.0006	0.0002	0.00055	0.00018	0.00037	-3.436
trichloroethylene	0.0055	0.0057	0.00504	0.00522	0.00513	-2.290
2-bromopropane	0.0033	0.0039	0.00302	0.00357	0.00330	-2.482
1,1,2,2-tetrachloroethane	0.0068	0.0069	0.00623	0.00632	0.00628	-2.202
carbon tetrachloride	0.0003	0.0004	0.00027	0.00037	0.00032	-3.494
cyclohexane	0.0033	0.004	0.00302	0.00367	0.00334	-2.476
1-bromobutane	0.0072	0.0019	0.00660	0.00174	0.00417	-2.380
bromoethane	0.0051	0.0048	0.00467	0.00440	0.00454	-2.343
1,2-dibromoethane	0.0069	0.0064	0.00632	0.00586	0.00609	-2.215
DMSO	---	---	---	---	---	---

Table VII: Solubility Data for p-toluic acid						
Solvent	Mass A	Mass B	Solubility A	Solubility B	Average Solubility	log Solubility
2-bromobutane	0.0802	0.0796	0.05891	0.05846	0.05869	-1.231
dibromomethane	0.1306	0.1244	0.09592	0.09137	0.09365	-1.029
1-bromopropane	0.099	0.1008	0.07271	0.07404	0.07337	-1.134
methylene chloride	0.1801	0.1799	0.13228	0.13213	0.13221	-0.879
1-chlorobutane	0.0757	0.0766	0.05560	0.05626	0.05593	-1.252
hexane	0.0123	0.0128	0.00903	0.00940	0.00922	-2.035
1,1,1-trichloroethane	0.0917	0.0915	0.06735	0.06721	0.06728	-1.172
tetrachloroethylene	0.0711	0.0703	0.05222	0.05163	0.05193	-1.285
trichloroethylene	0.1848	0.1844	0.13573	0.13544	0.13559	-0.868
2-bromopropane	0.0767	0.0764	0.05633	0.05611	0.05622	-1.250
1,1,2,2-tetrachloroethane	0.1376	0.1344	0.10107	0.09871	0.09989	-1.000
carbon tetrachloride	0.0636	0.0637	0.04671	0.04679	0.04675	-1.330
cyclohexane	0.0154	0.0152	0.01131	0.01116	0.01124	-1.949
1-bromobutane	0.0844	0.0836	0.06199	0.06140	0.06170	-1.210
bromoethane	0.1102	0.1109	0.08094	0.08145	0.08120	-1.090
1,2-dibromoethane	0.086	0.0896	0.06317	0.06581	0.06449	-1.191
DMSO	---	---	---	---	---	---

Figure 1: UV-vis Spectrum for 2-bromobutane

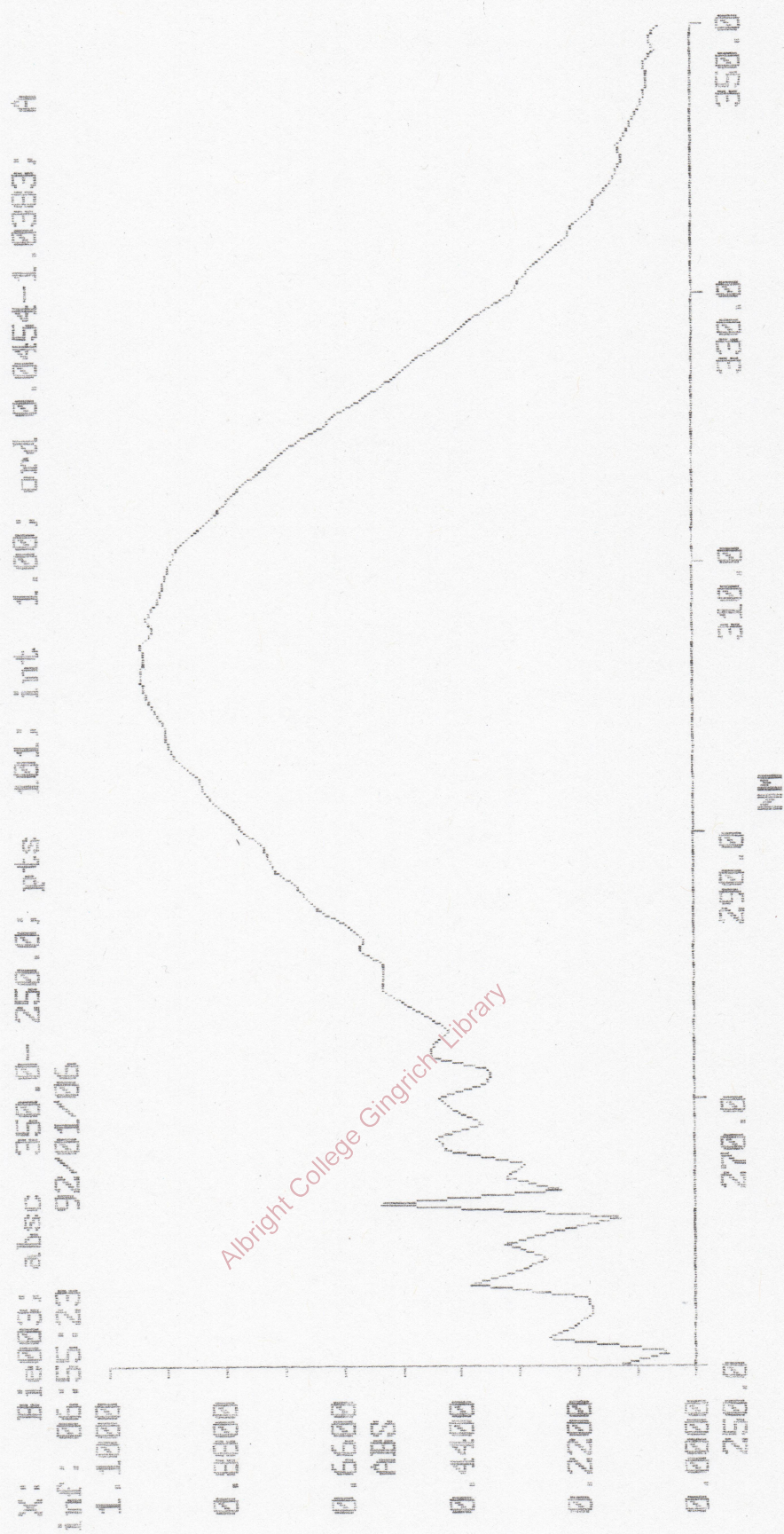


Figure 2: UV-vis Spectrum for 2-bromopropane

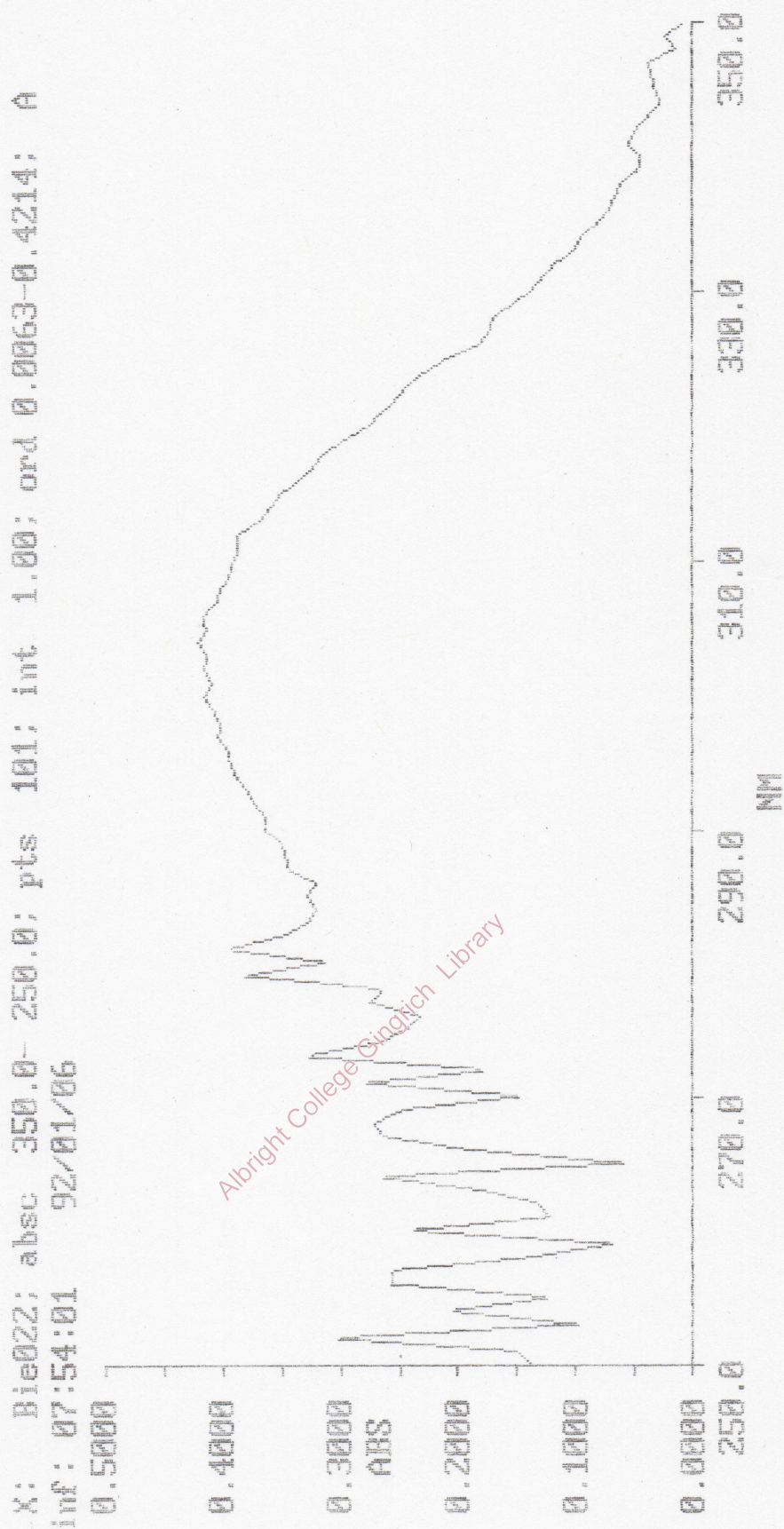


Figure 3: UV-vis Spectrum for 1,1,2,2-tetrachloroethane

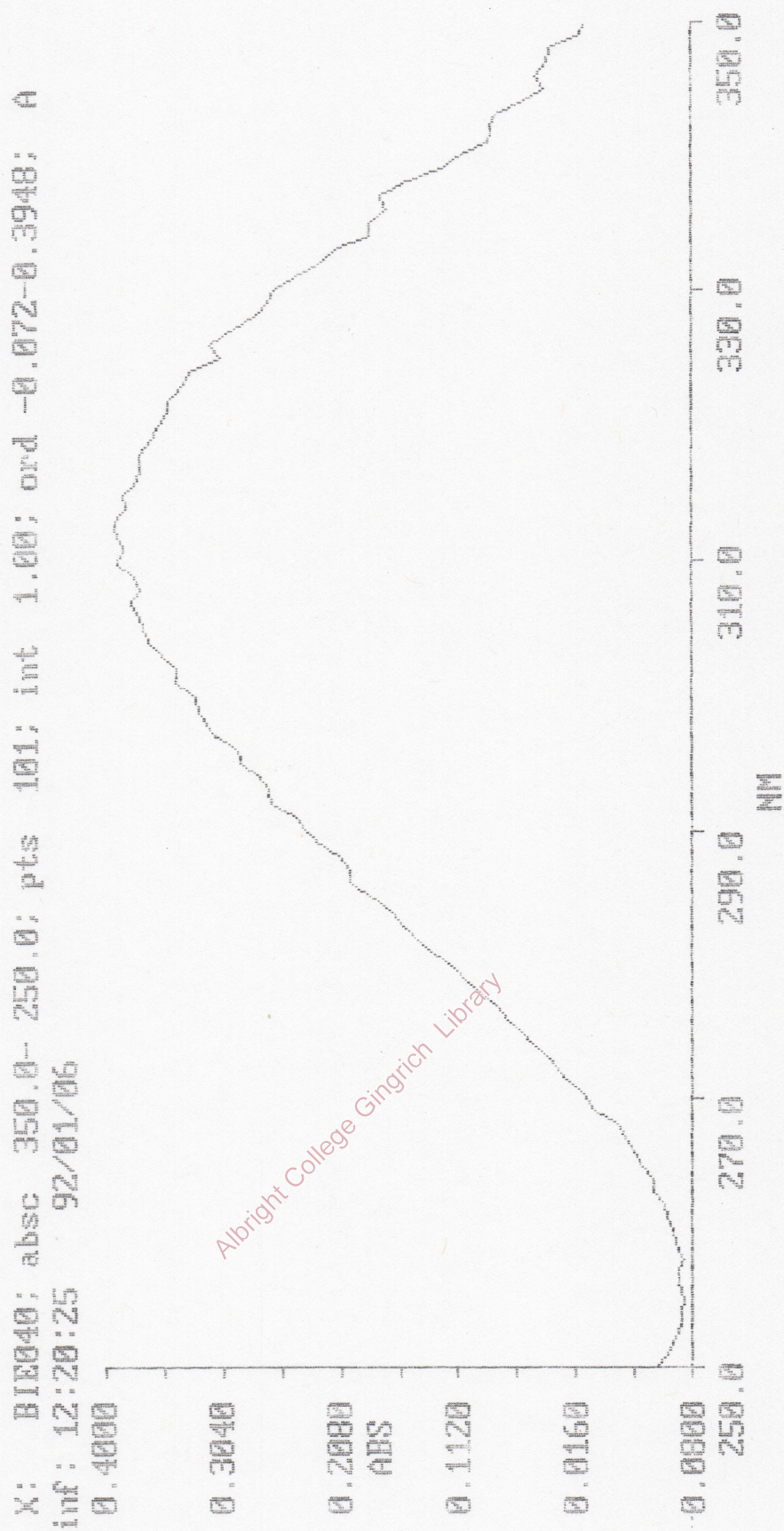


Figure 4: UV-vis Spectrum for 1,1,2,2-tetrachloroethane (rescan)

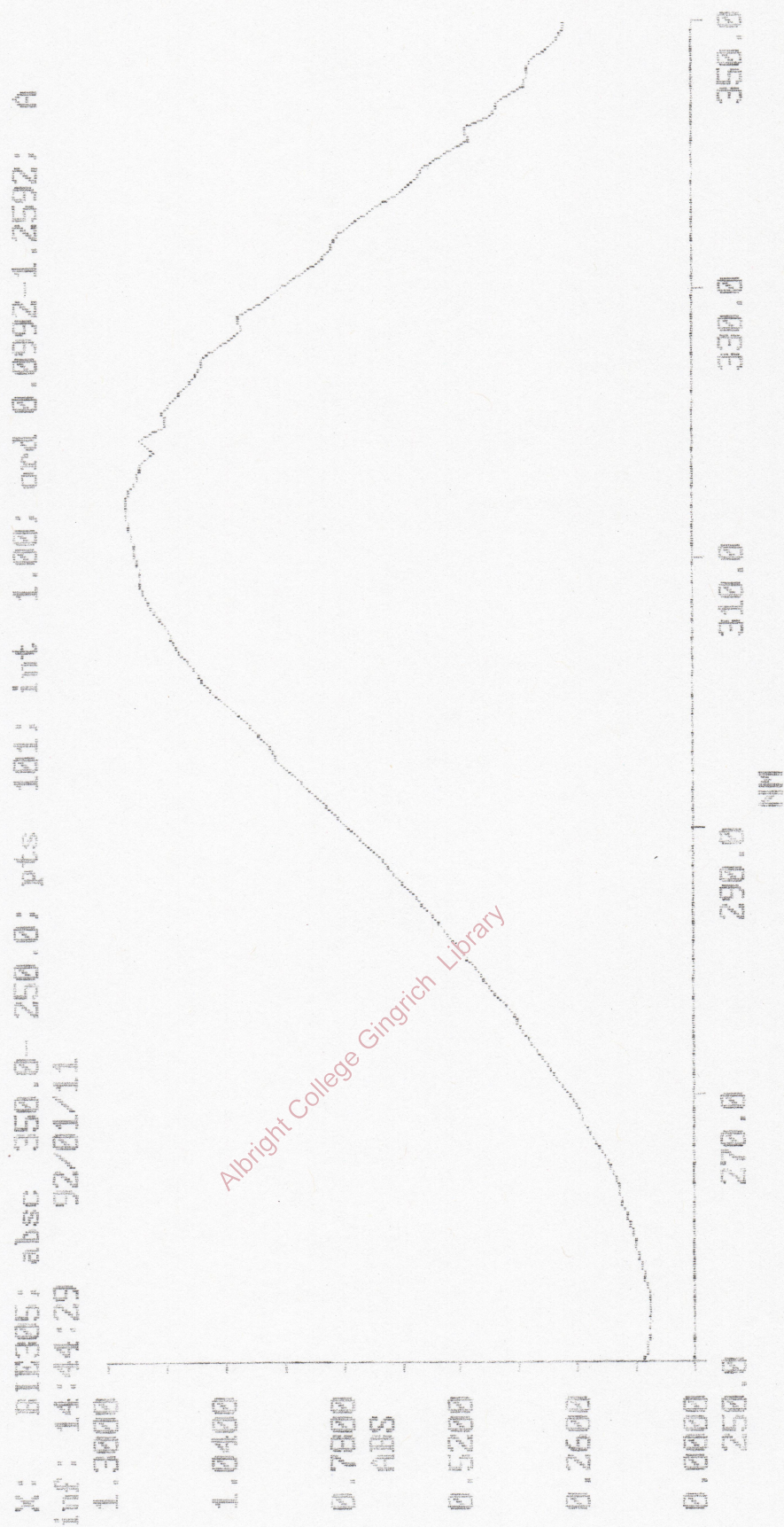


Figure 5: UV-vis Spectrum for 1,1,1-trichloroethane

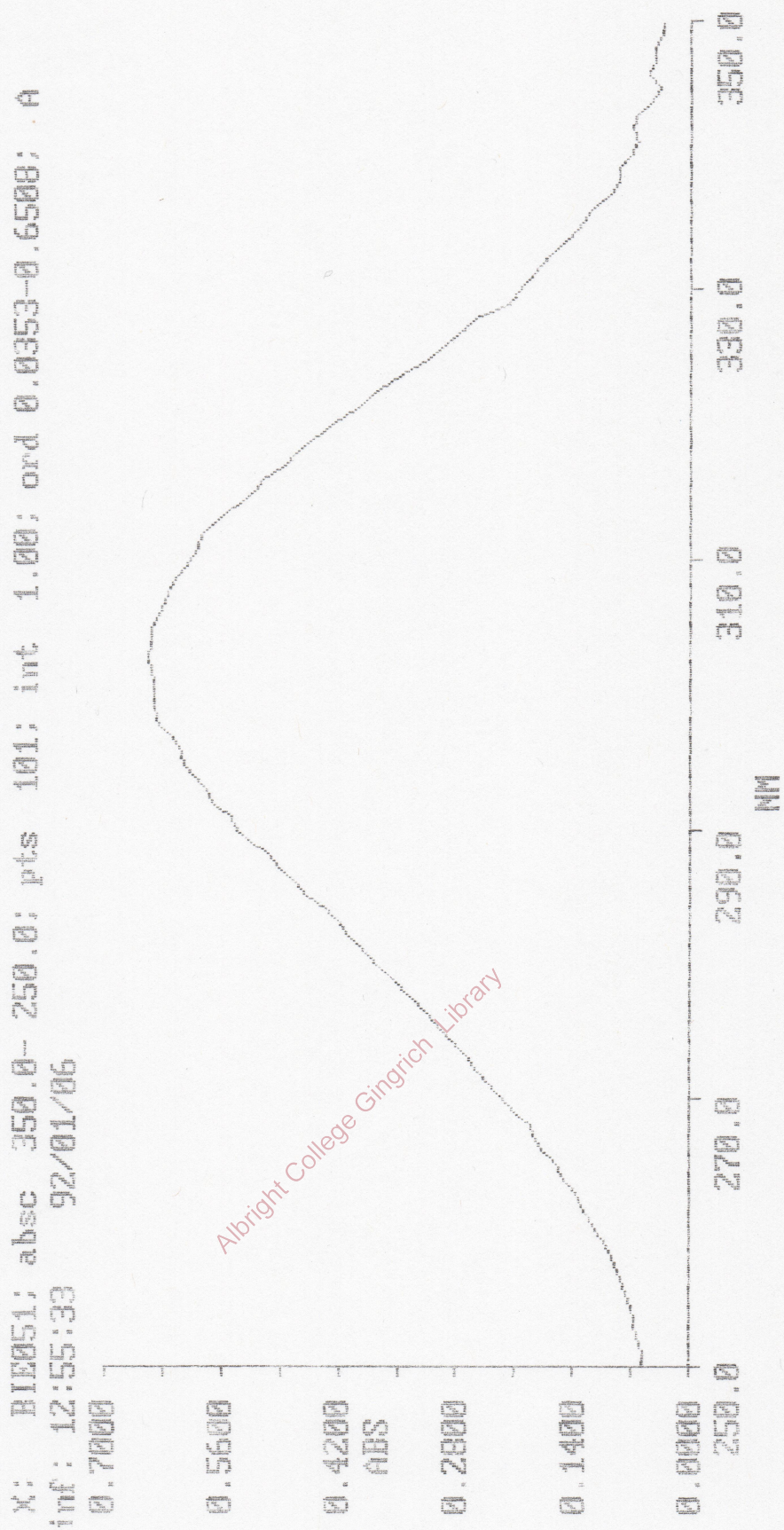


Figure 6: UV-vis Spectrum for 1-chlorobutane

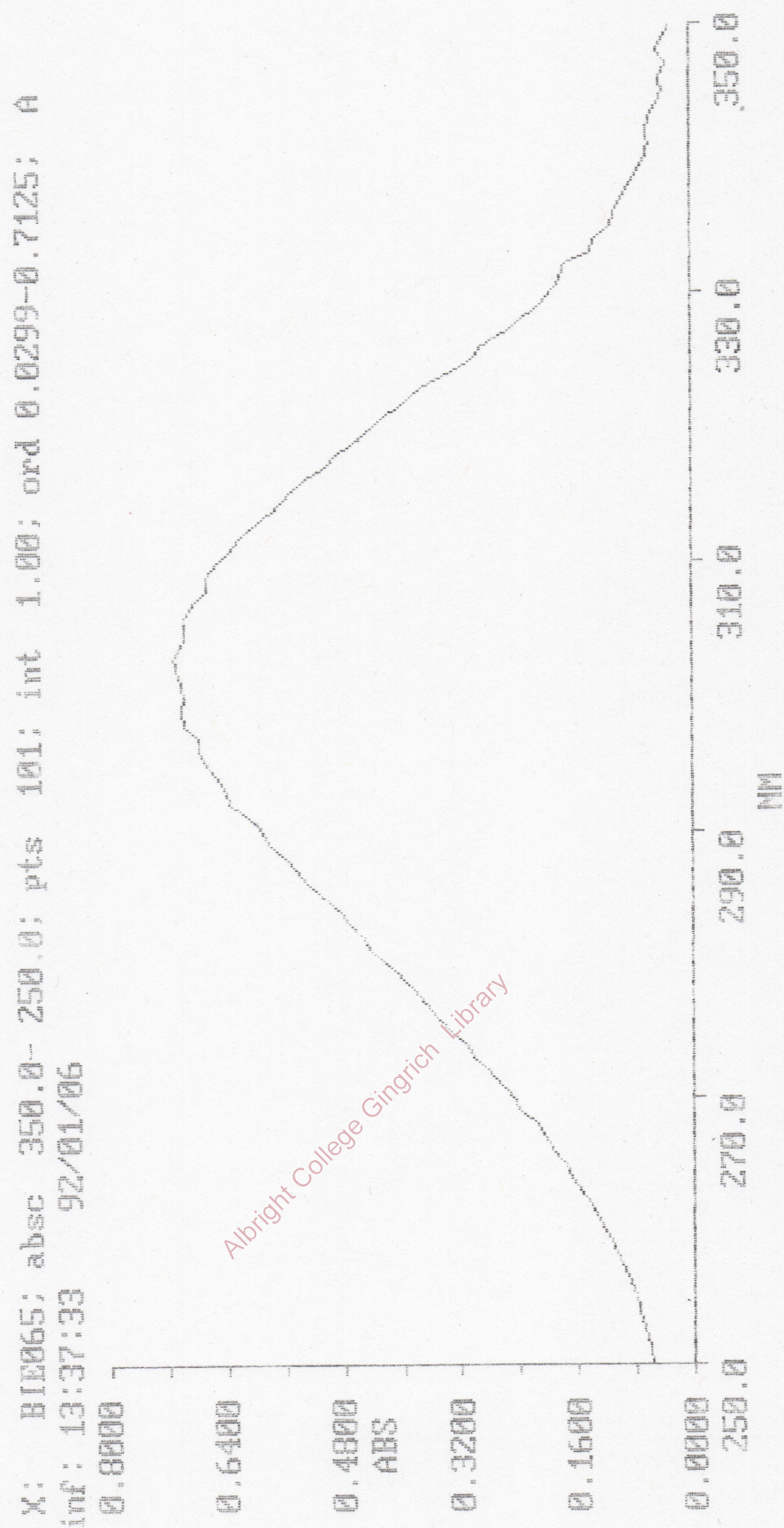


Figure 7: UV-vis Spectrum for 1-chlorobutane (rescan)

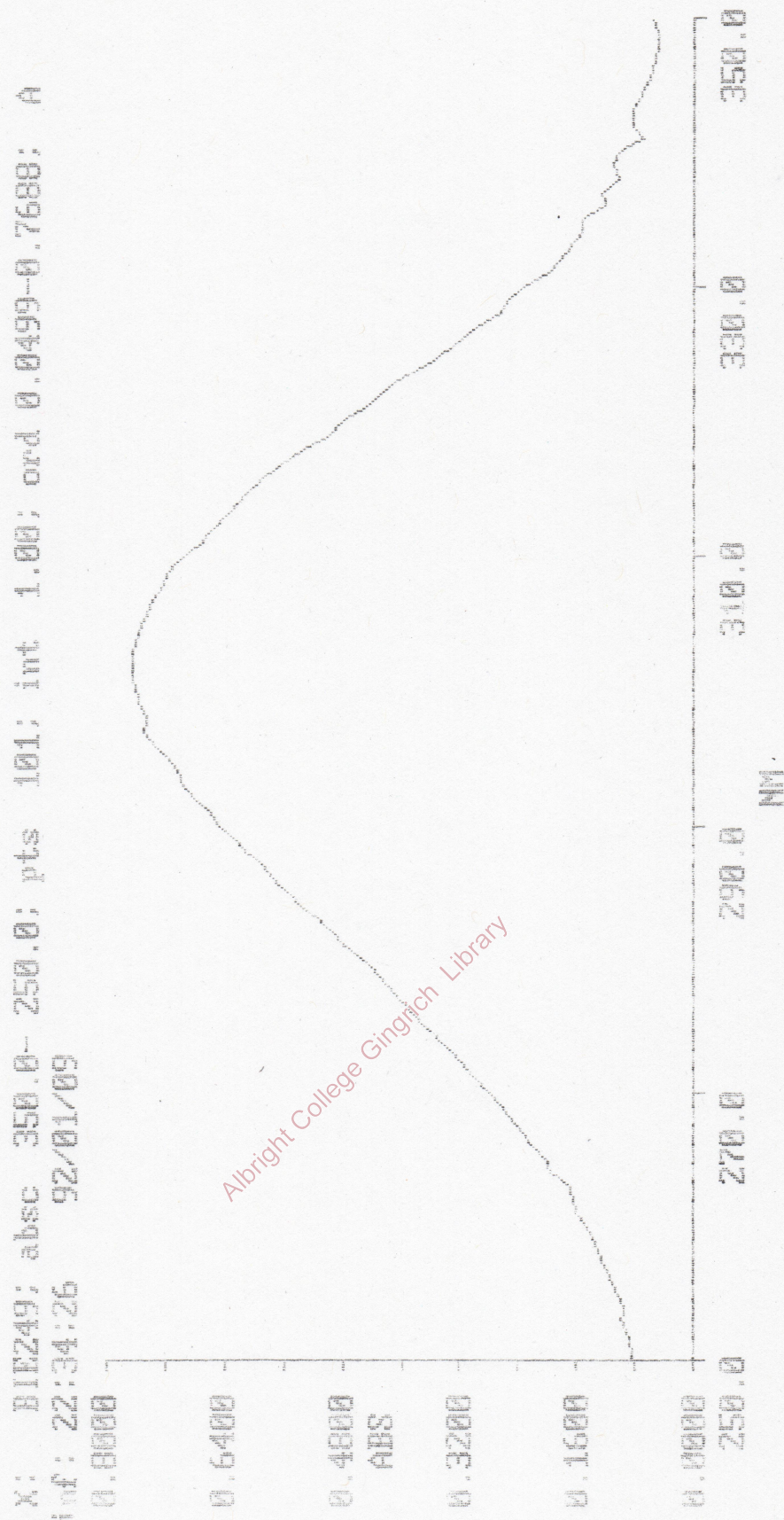


Figure 8: UV-vis Spectrum for Cyclohexane

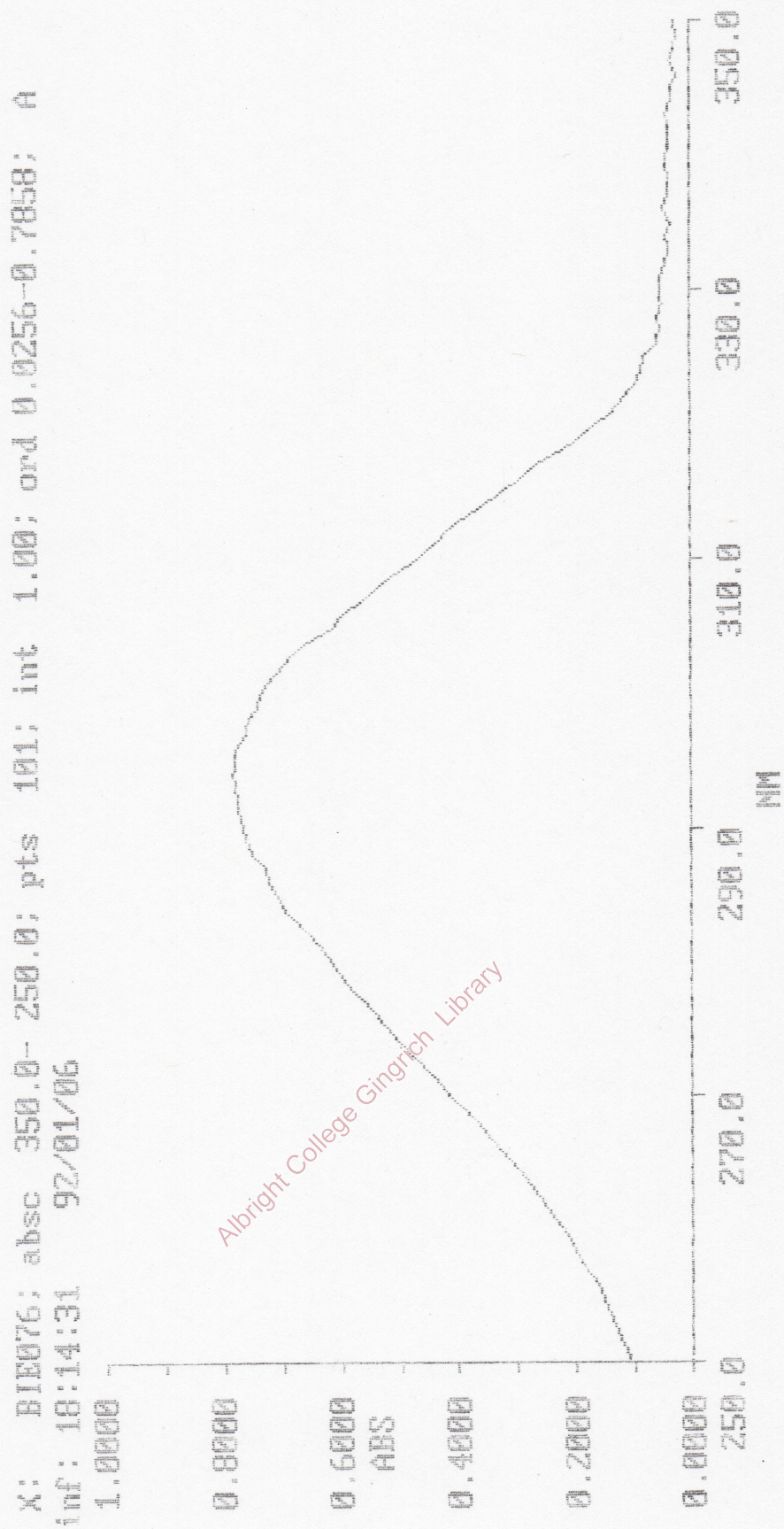


Figure 9: UV-vis Spectrum for 1-bromopropane

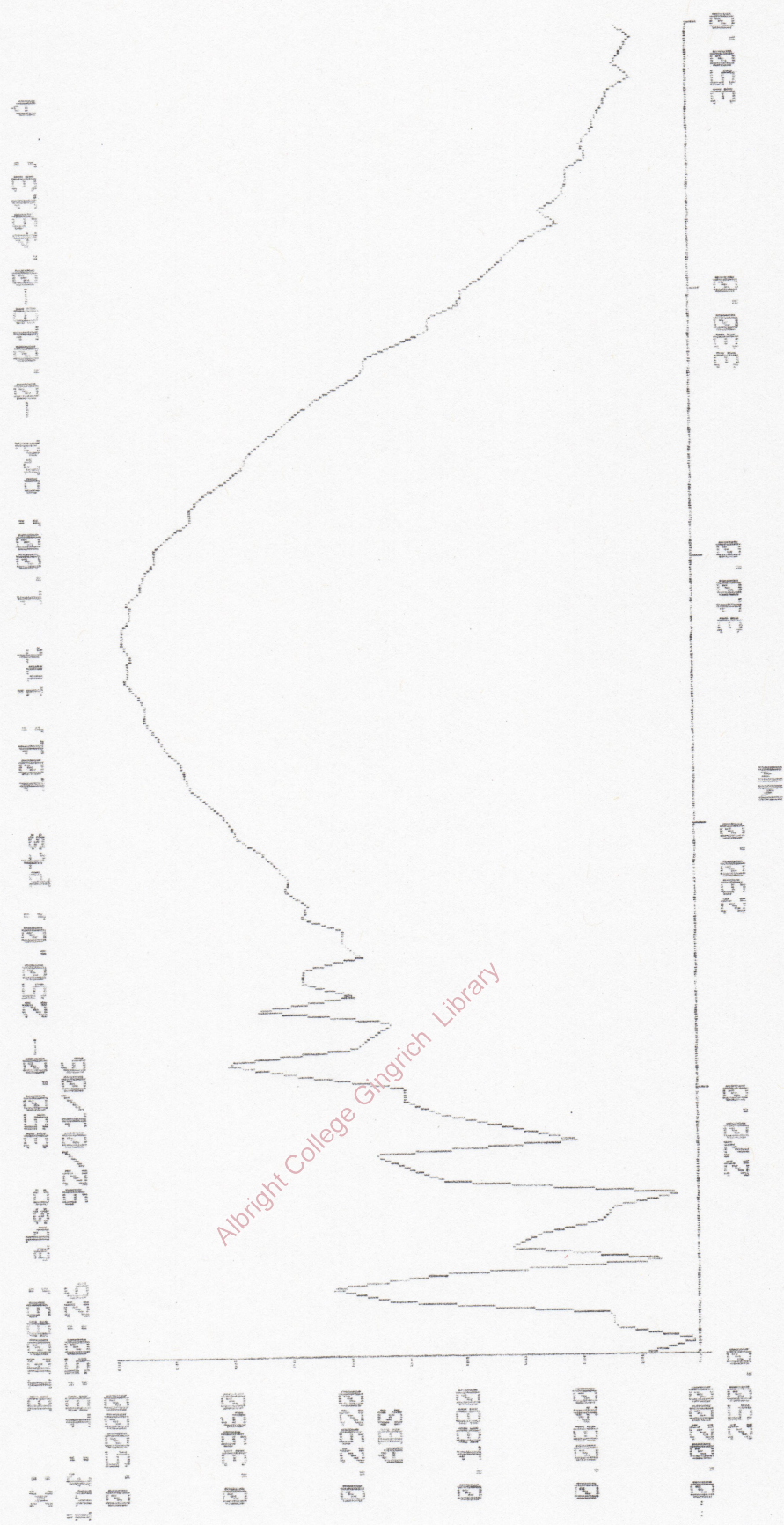


Figure 10: UV-vis Spectrum for Trichloroethylene

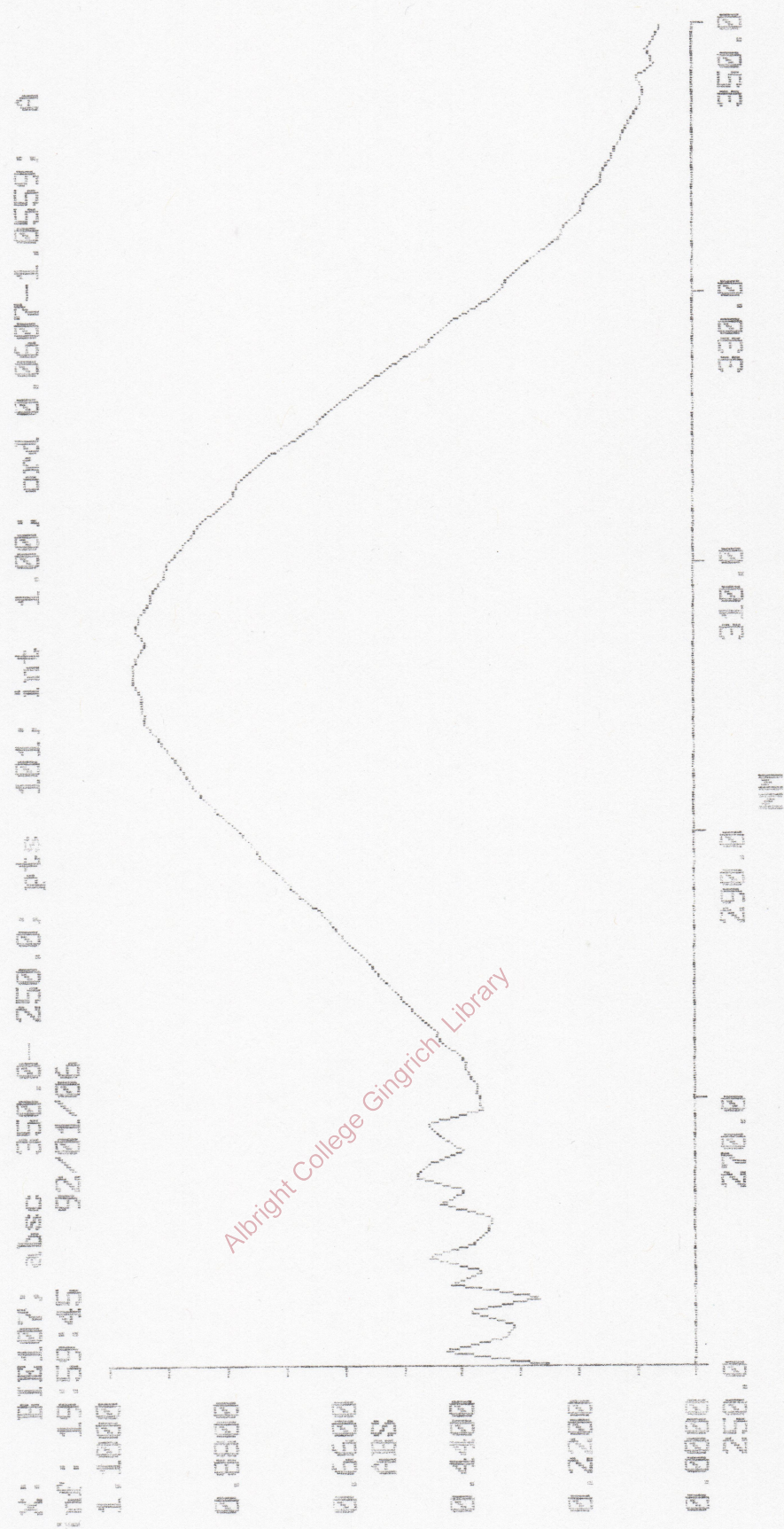


Figure 11: UV-vis Spectrum for Dibromomethane

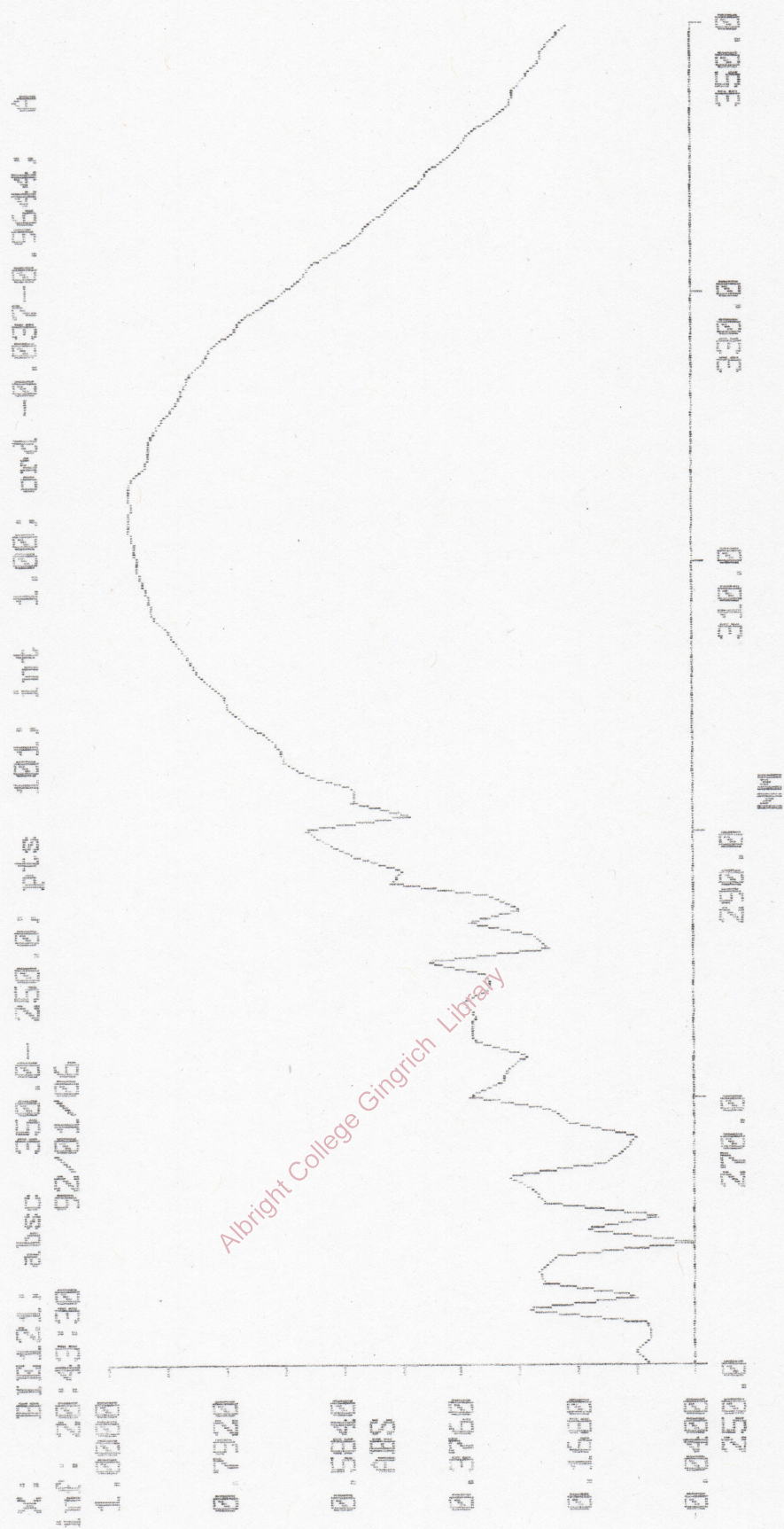


Figure 12: UV-vis Spectrum for Dibromomethane (rescan)

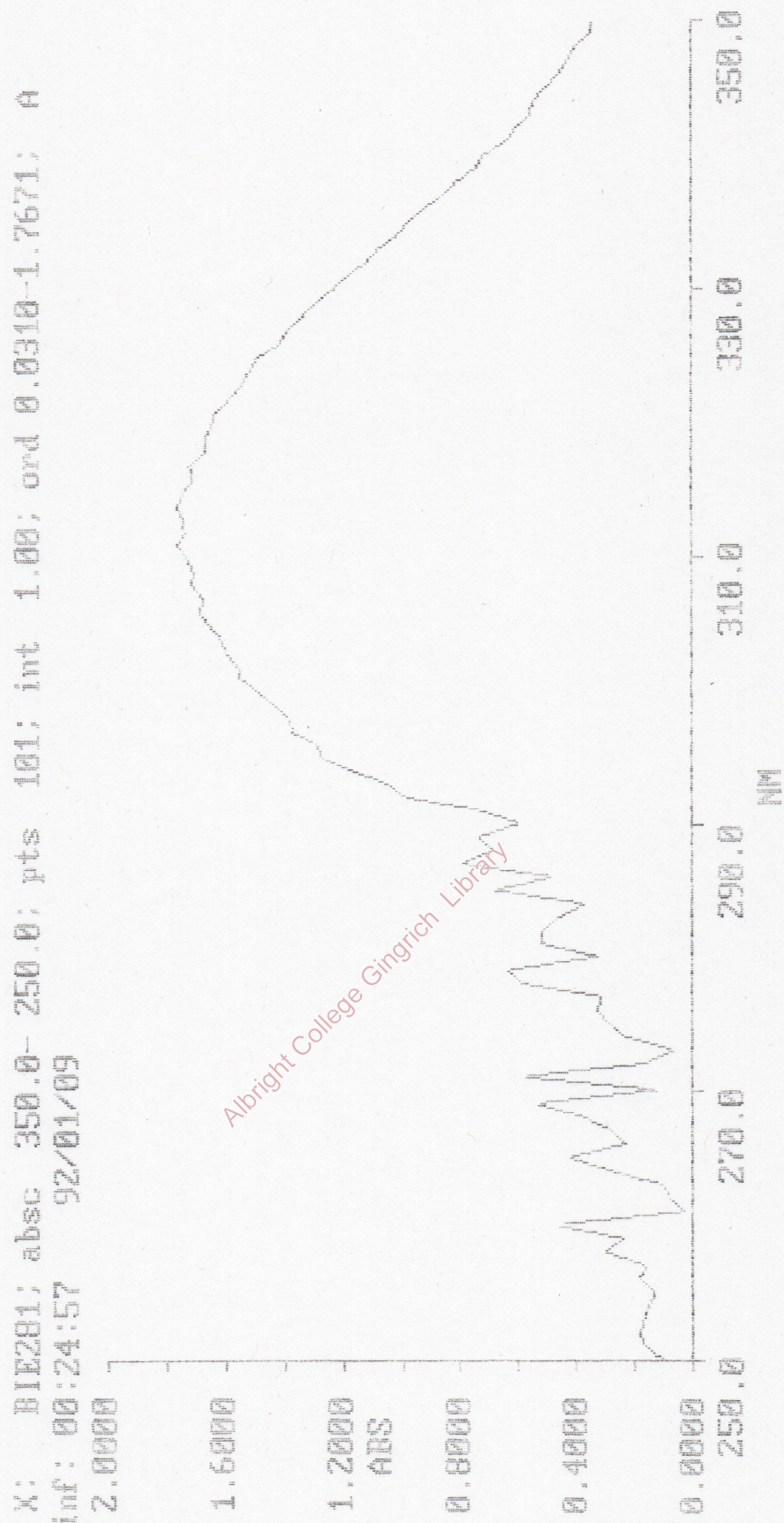


Figure 13: UV-vis Spectrum for Methylene Chloride

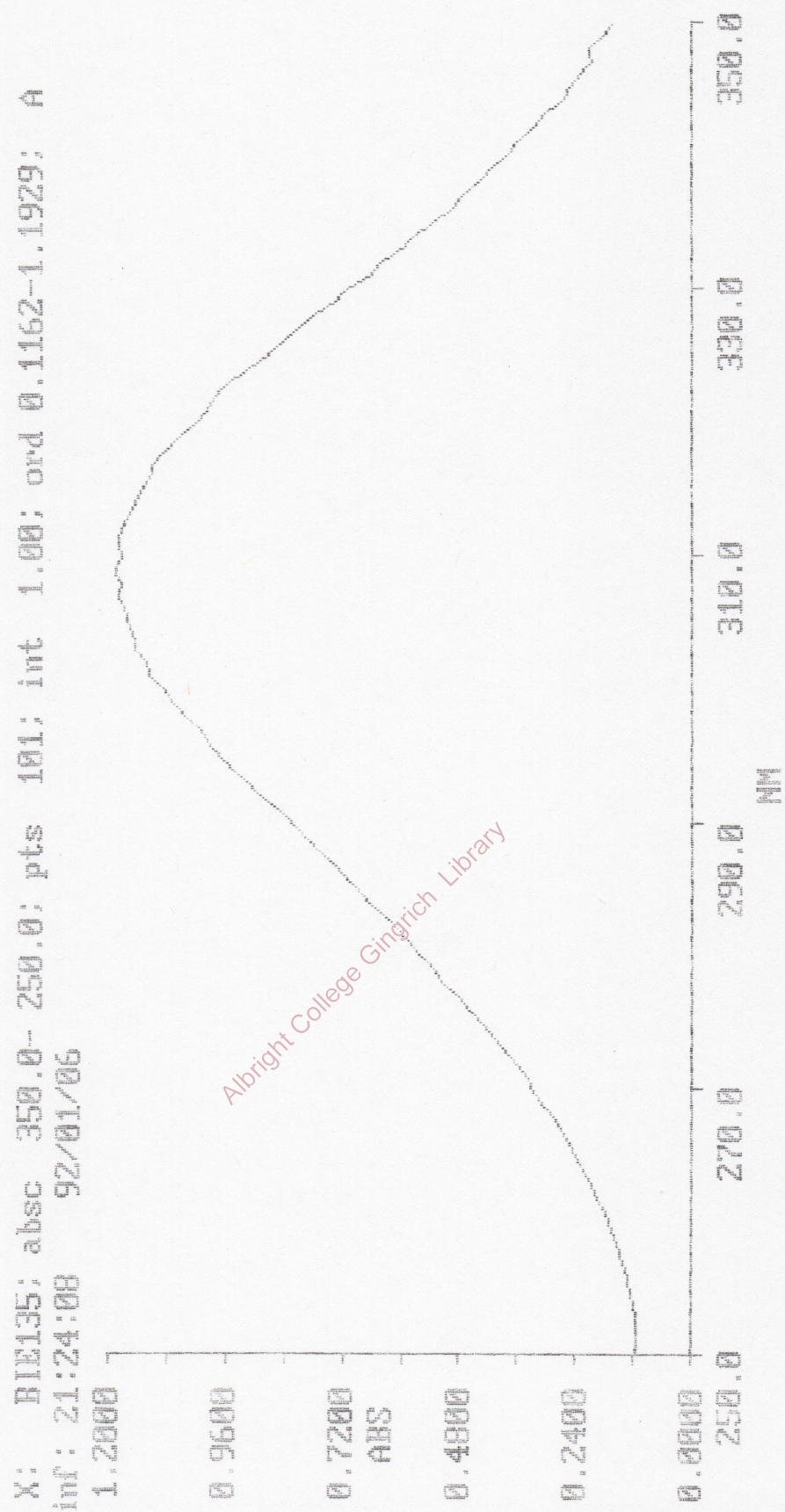


Figure 14: UV-vis Spectrum for Hexanes

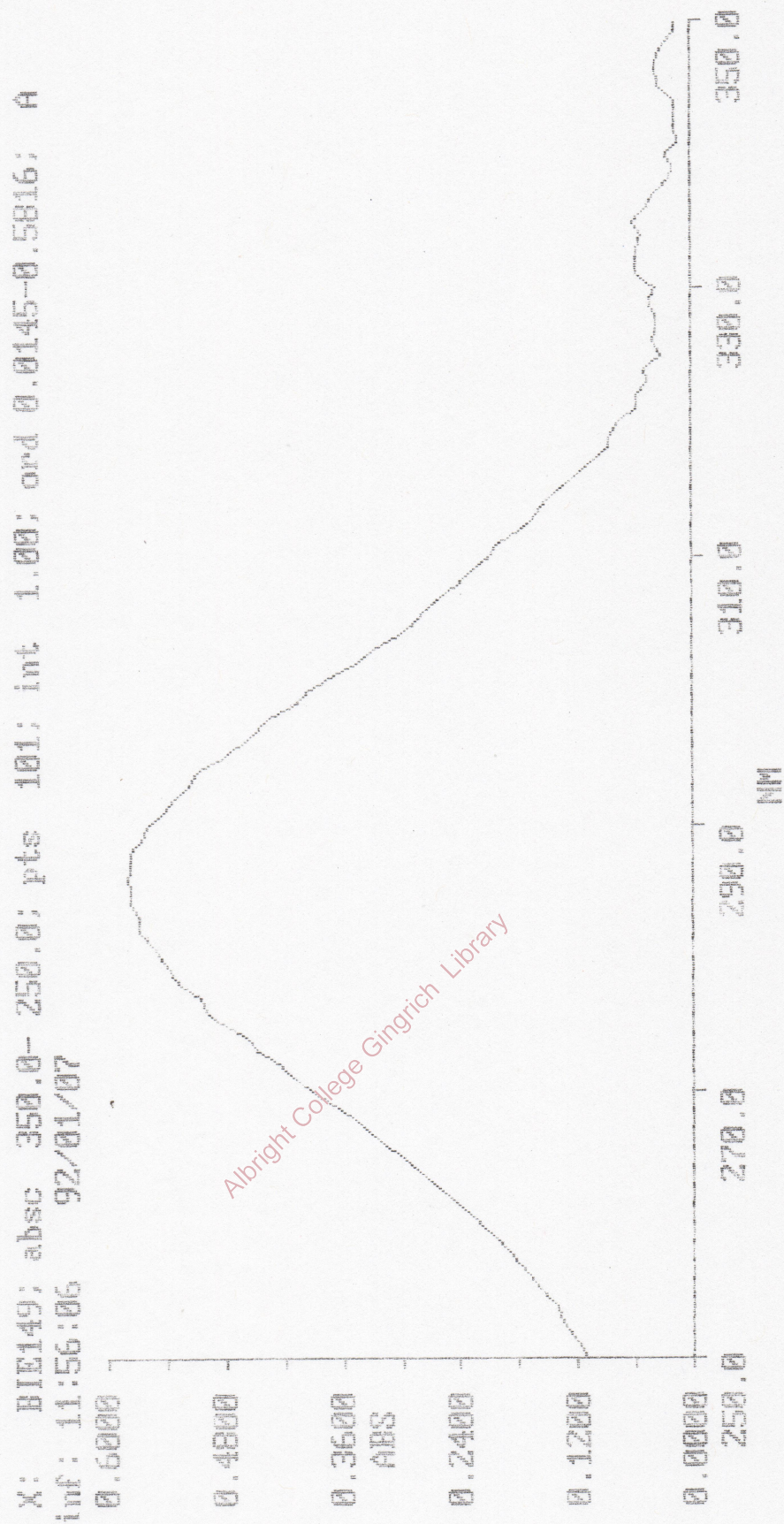


Figure 15: UV-vis Spectrum for Tetrachloroethylene

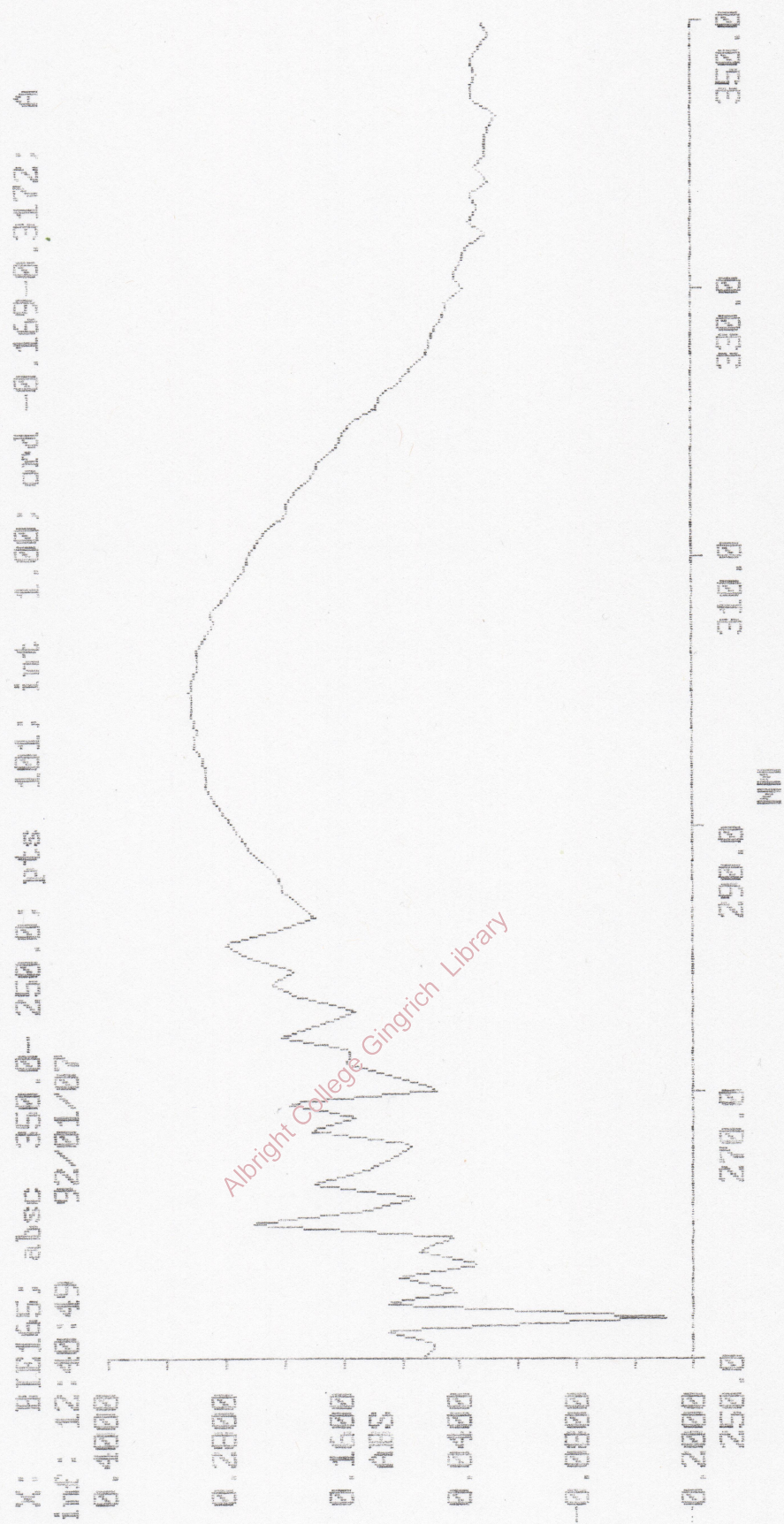


Figure 16: UV-vis Spectrum for 1-bromobutane

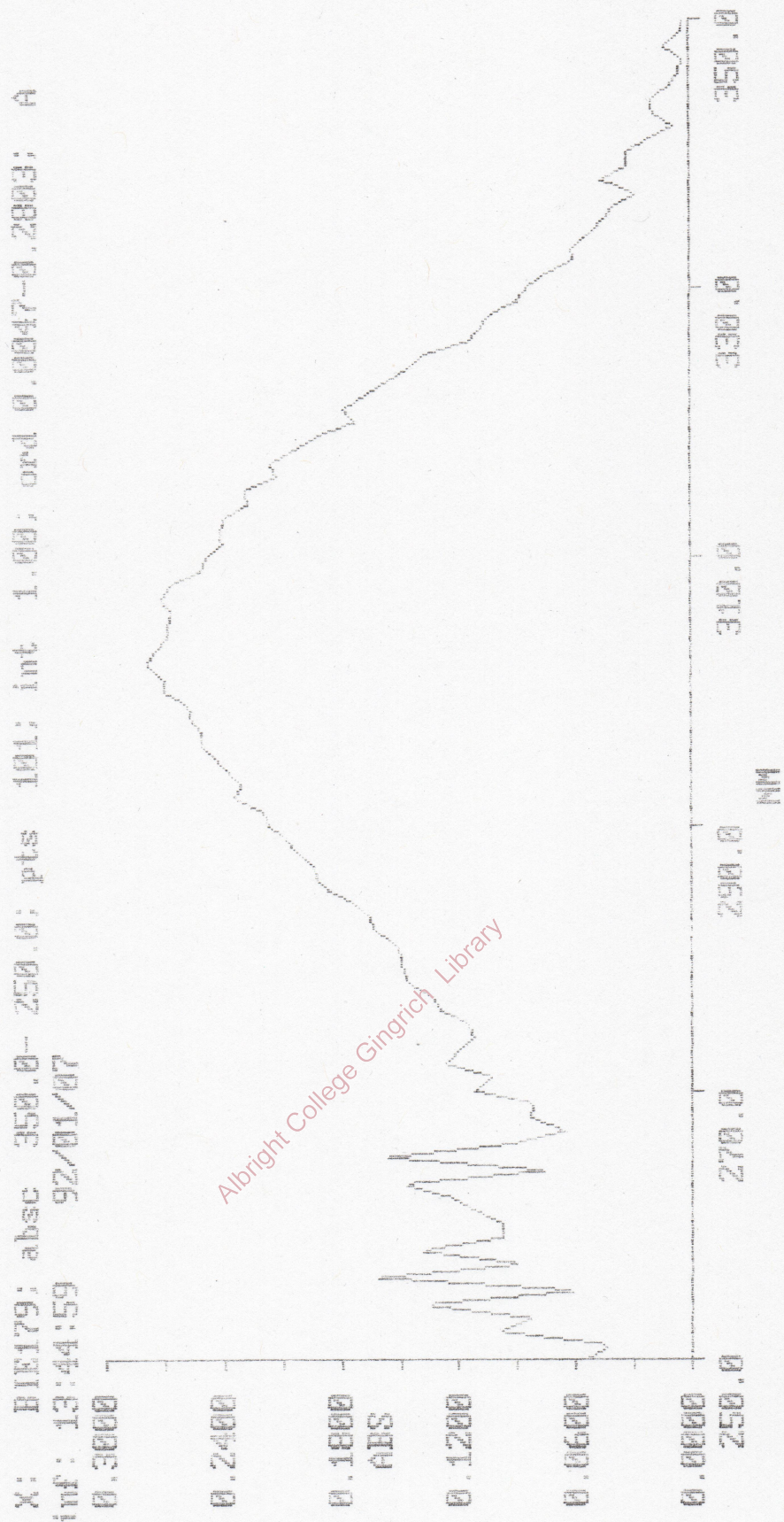


Figure 17: UV-vis Spectrum for Bromoethane

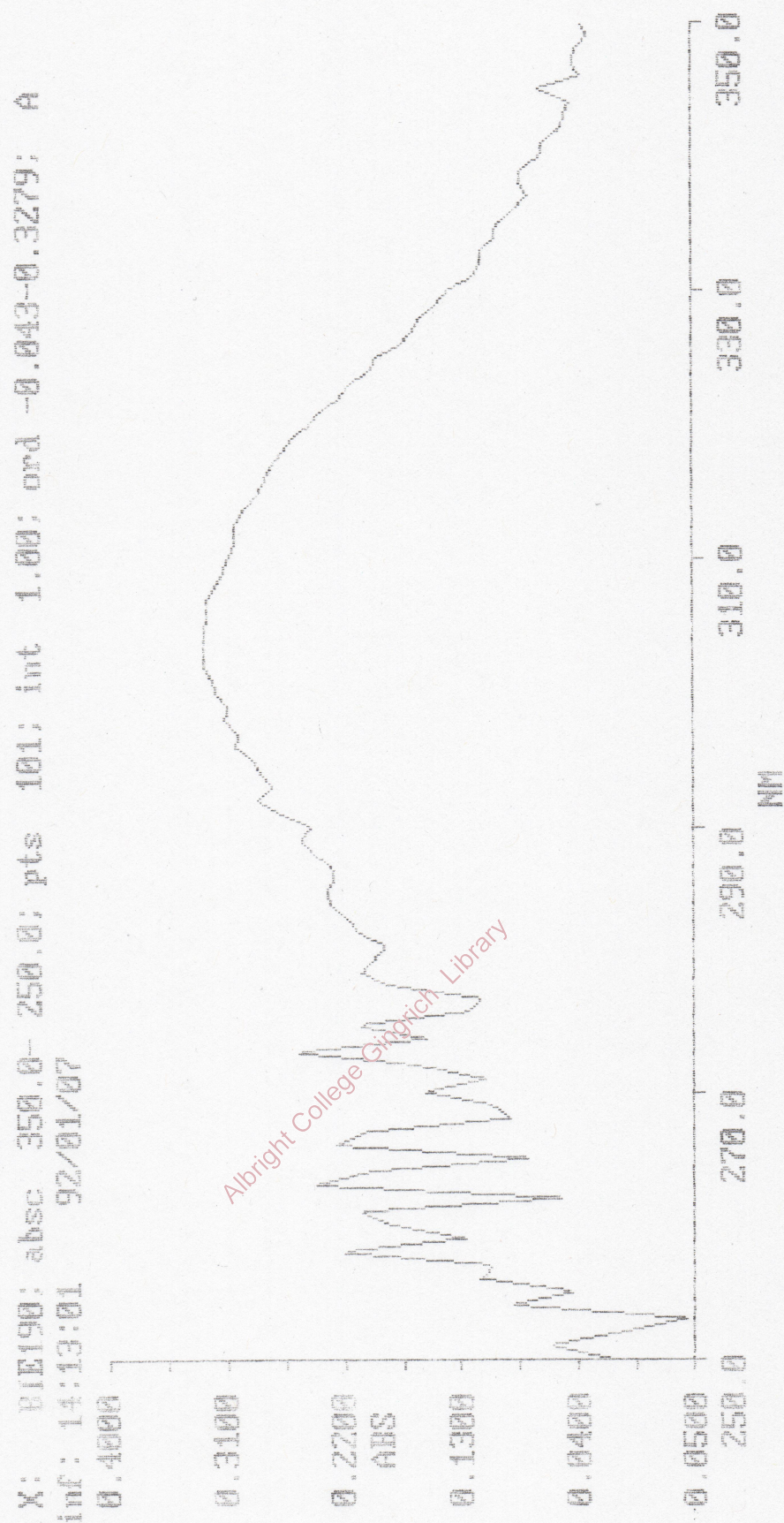


Figure 18: UV-vis Spectrum for Bromoethane (rescan)

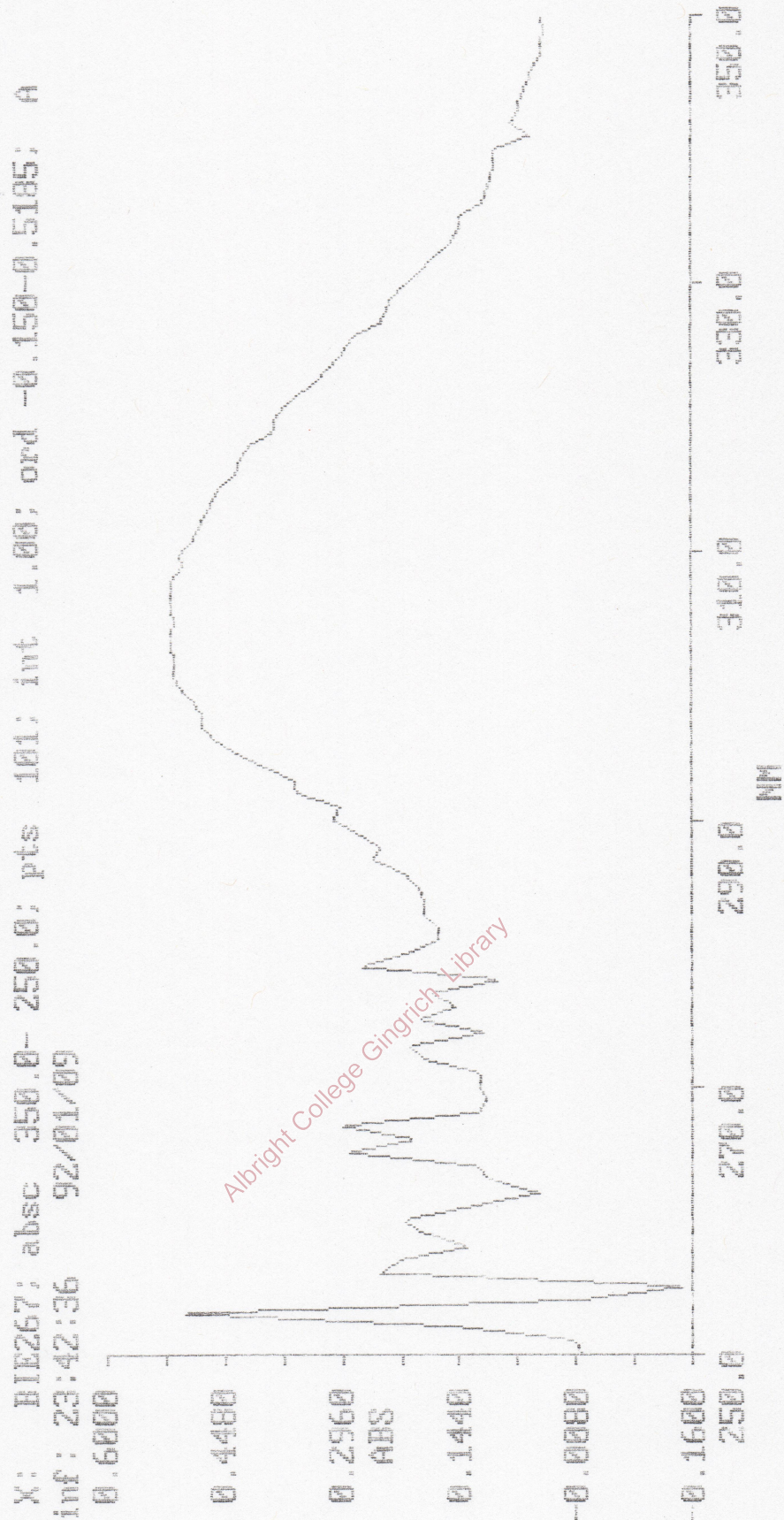


Figure 19: UV-vis Spectrum for 1,2-dibromoethane

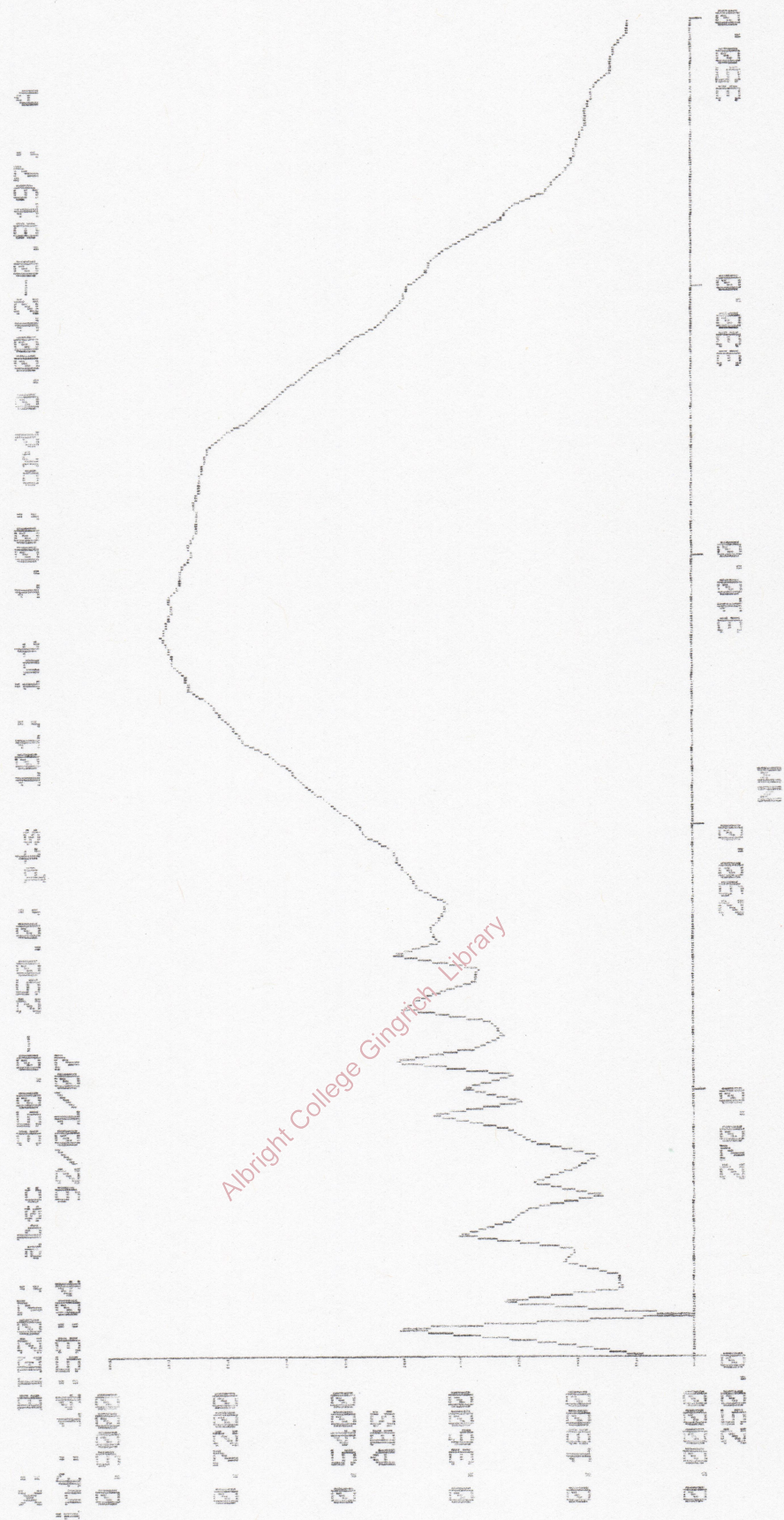


Figure 20: UV-vis Spectrum for 1,2-dibromoethane (rescan)

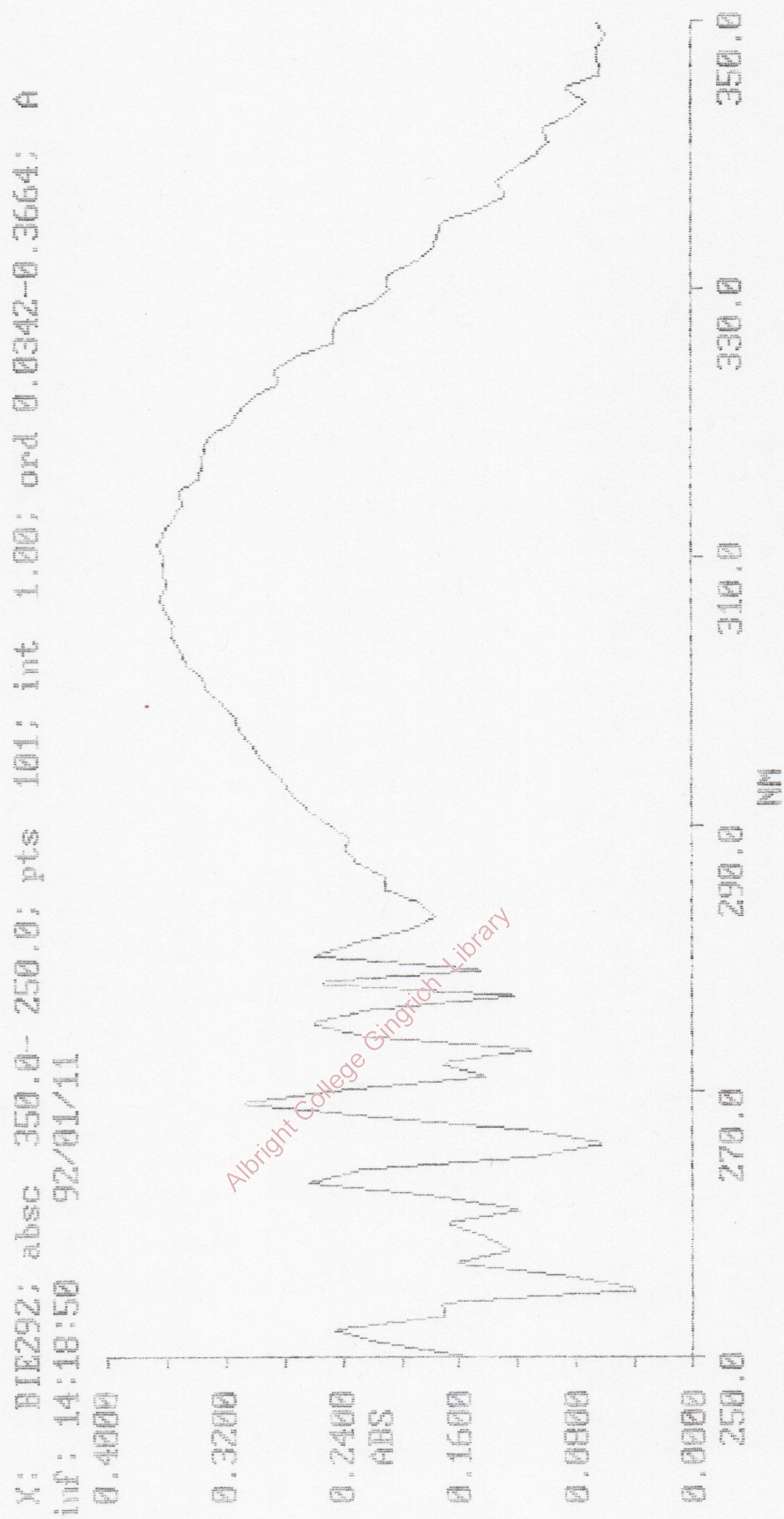


Figure 21: UV-vis Spectrum for Carbon tetrachloride

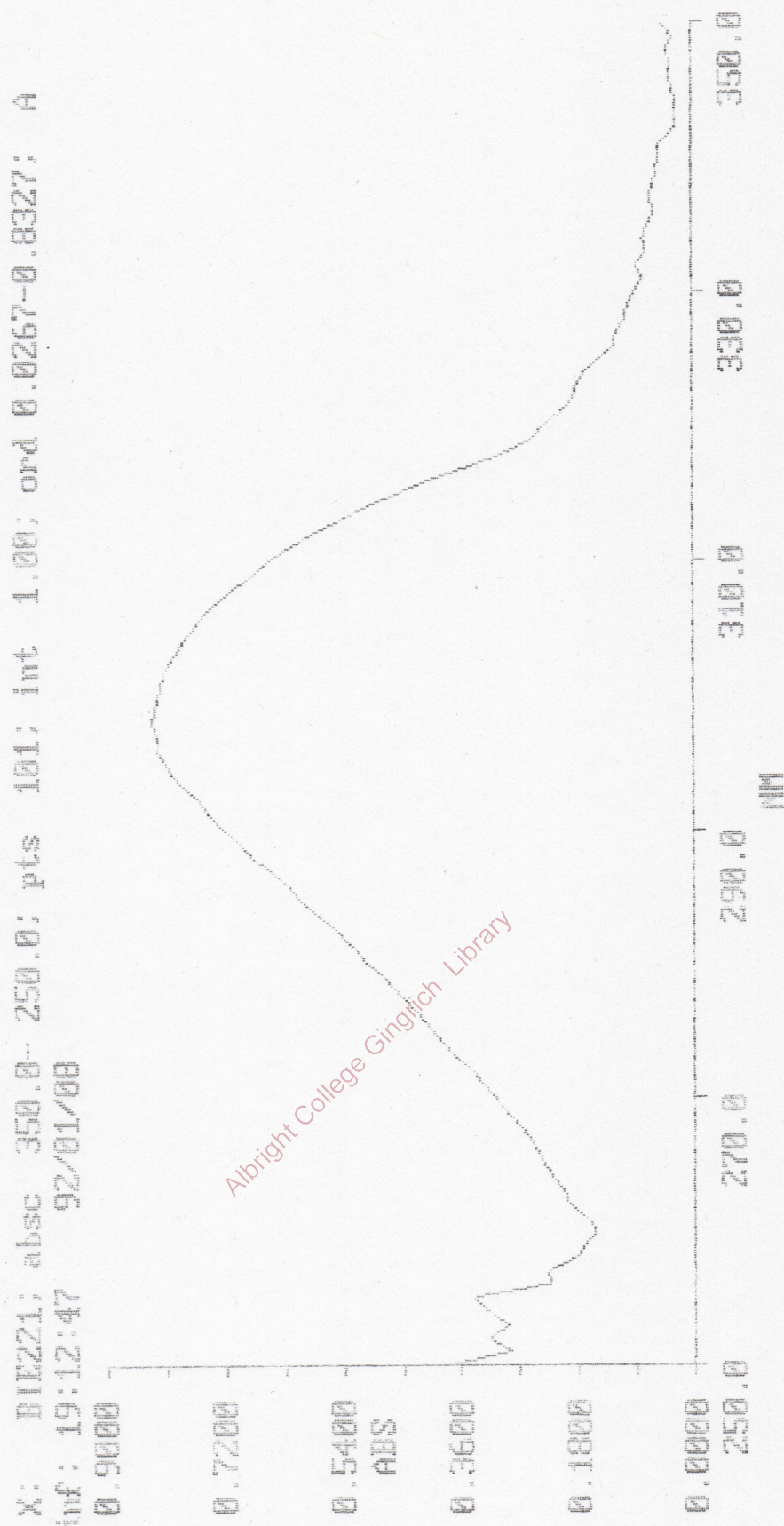


Figure 22: UV-vis Spectrum for DMSO

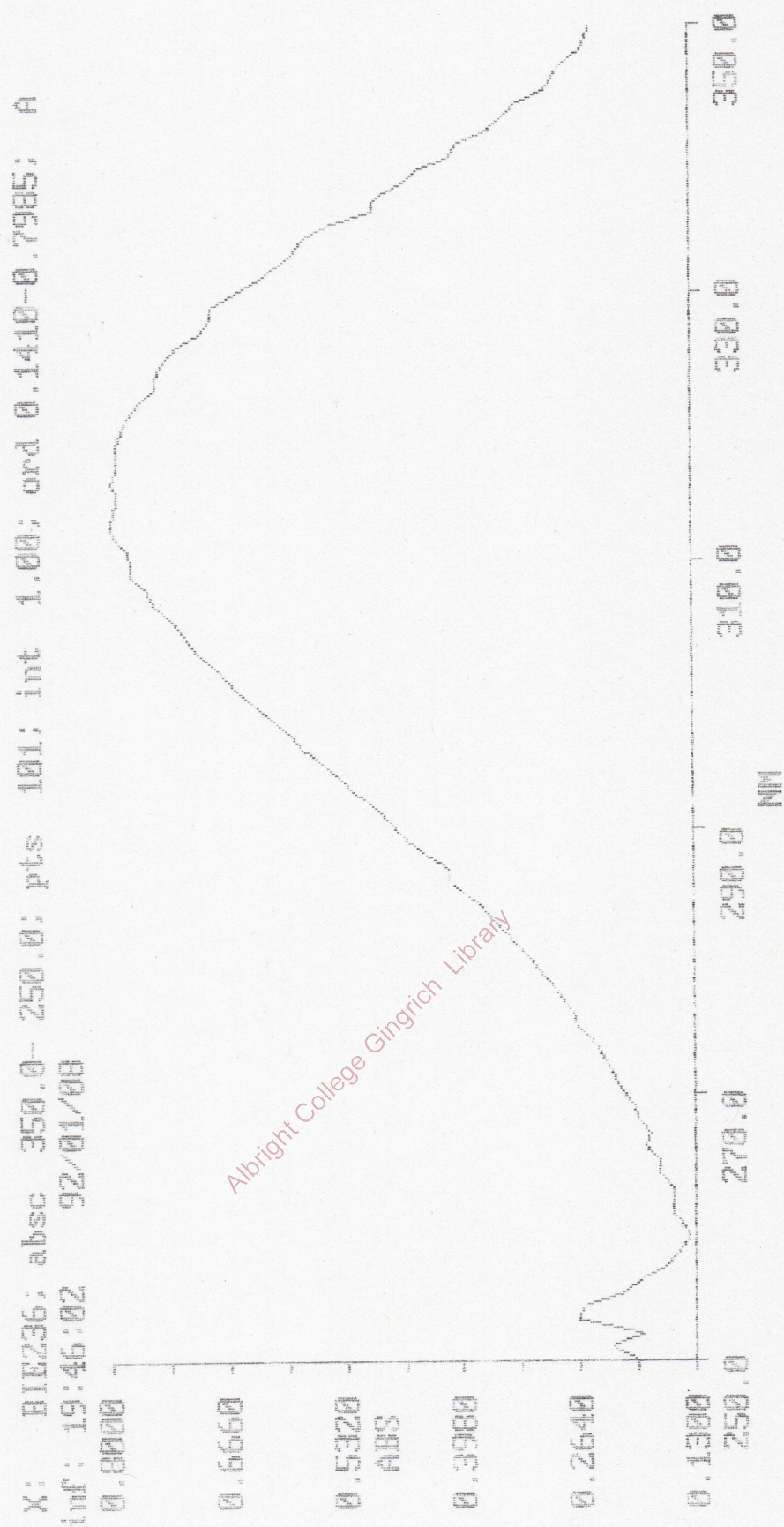
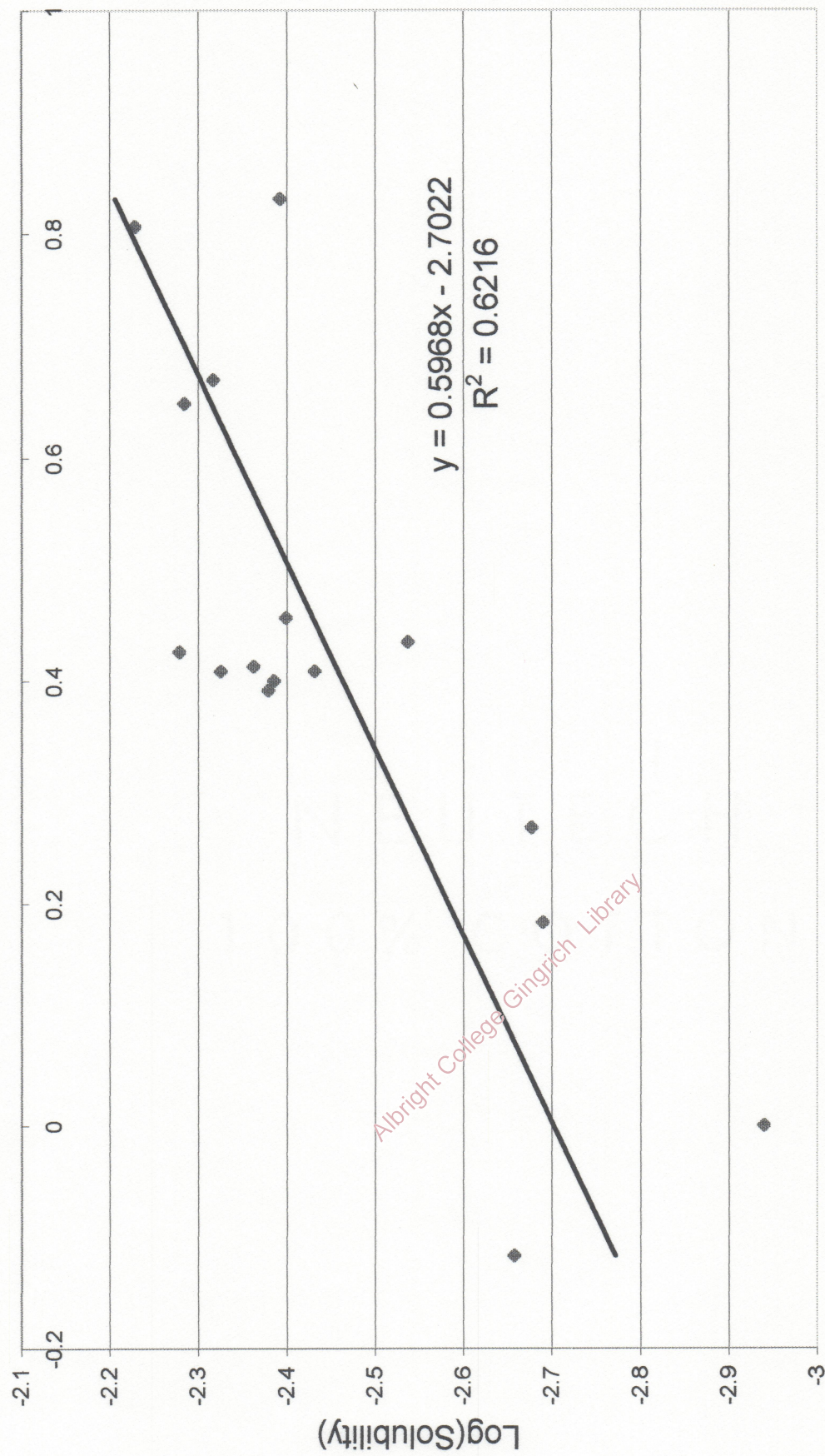
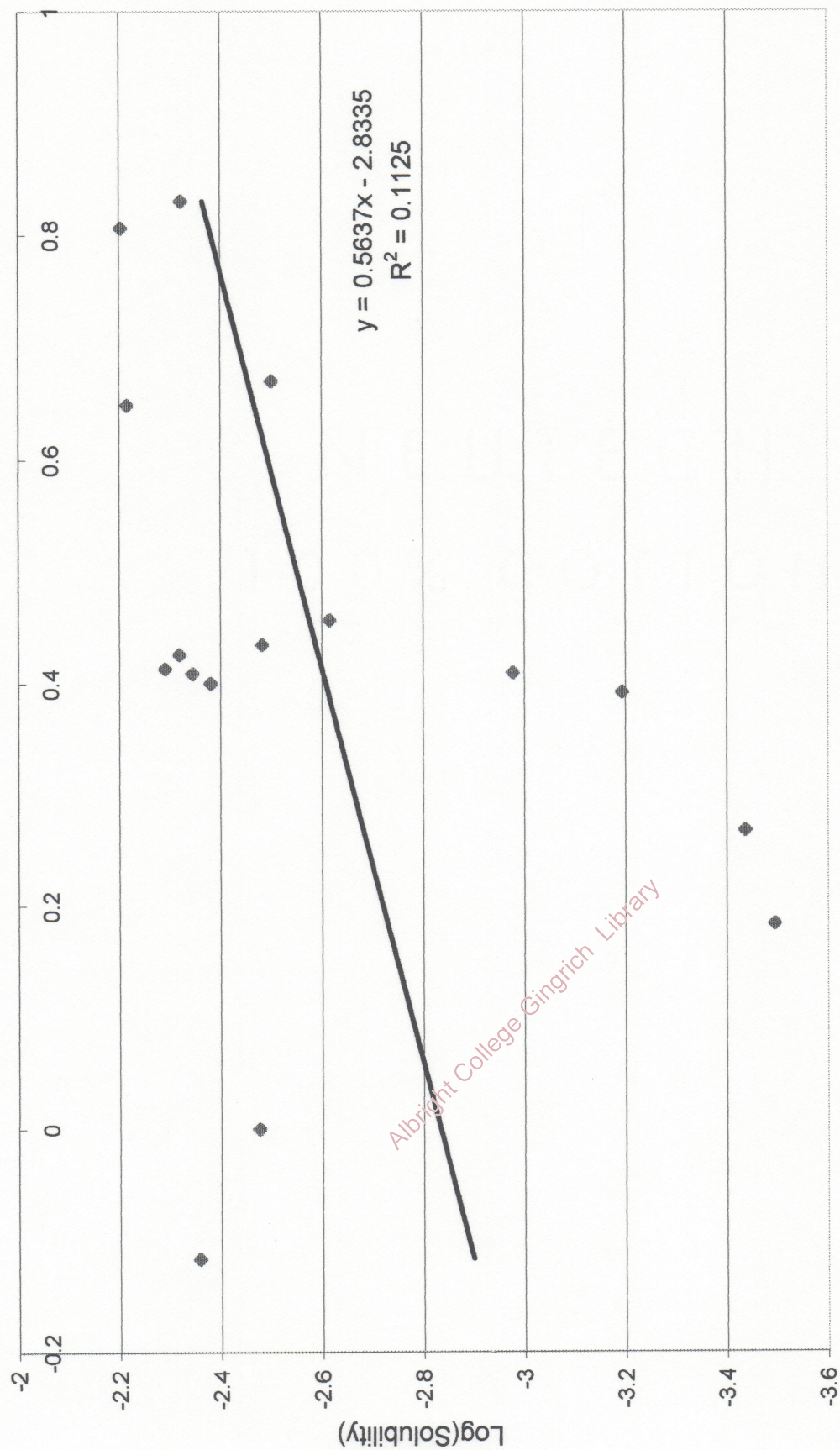


Figure 23: Pi Star vs. Log(Solubility) of p-chlorobenzoic Acid



Pi Star

Figure 24: Pi Star vs. Log(Solubility) of p-aminophenol



Pi Star

Figure 25: Pi Star vs. Log(Solubility) of Toluic Acid

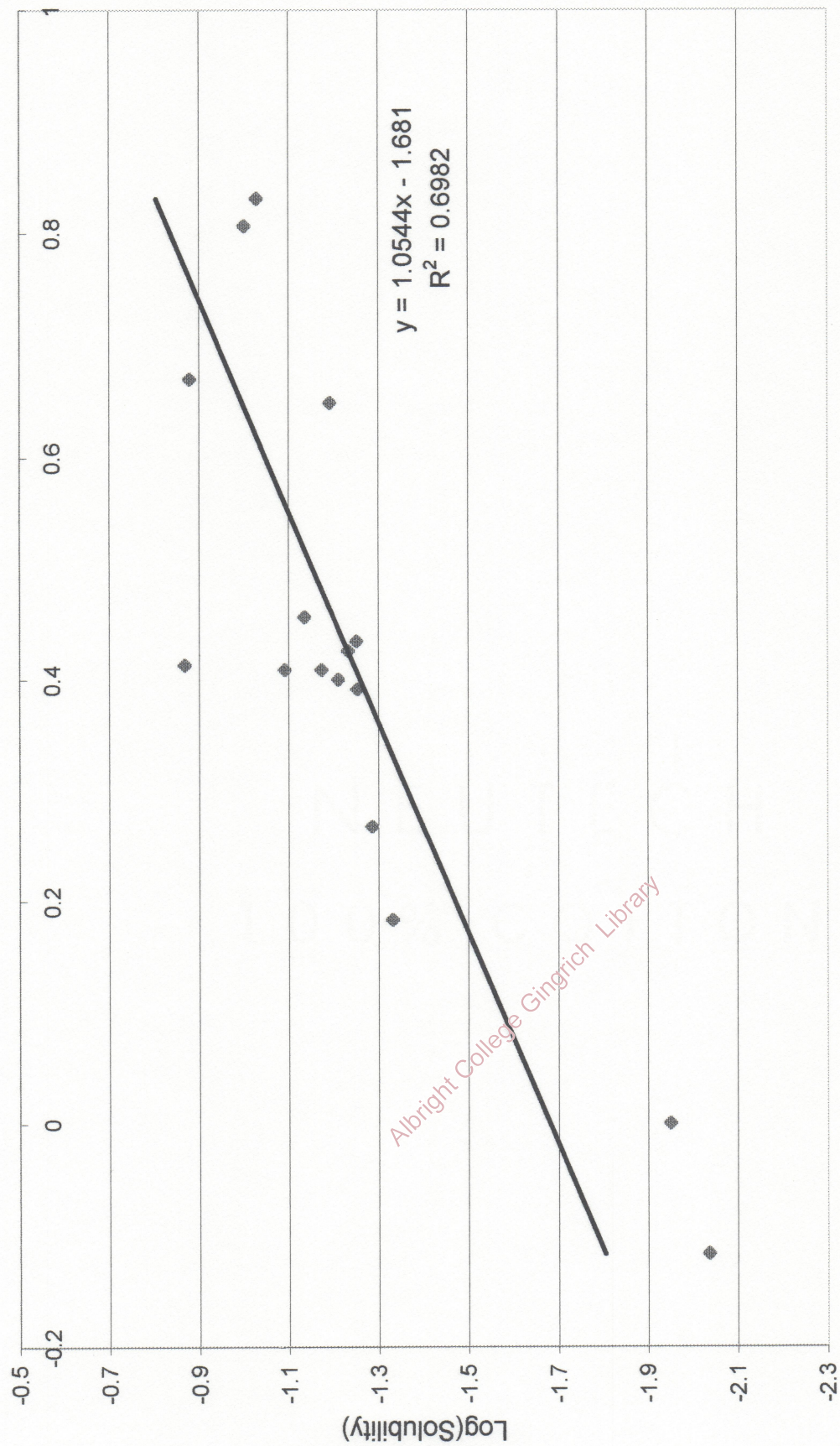


Figure 26: Pi Star vs. Log(Solubility)

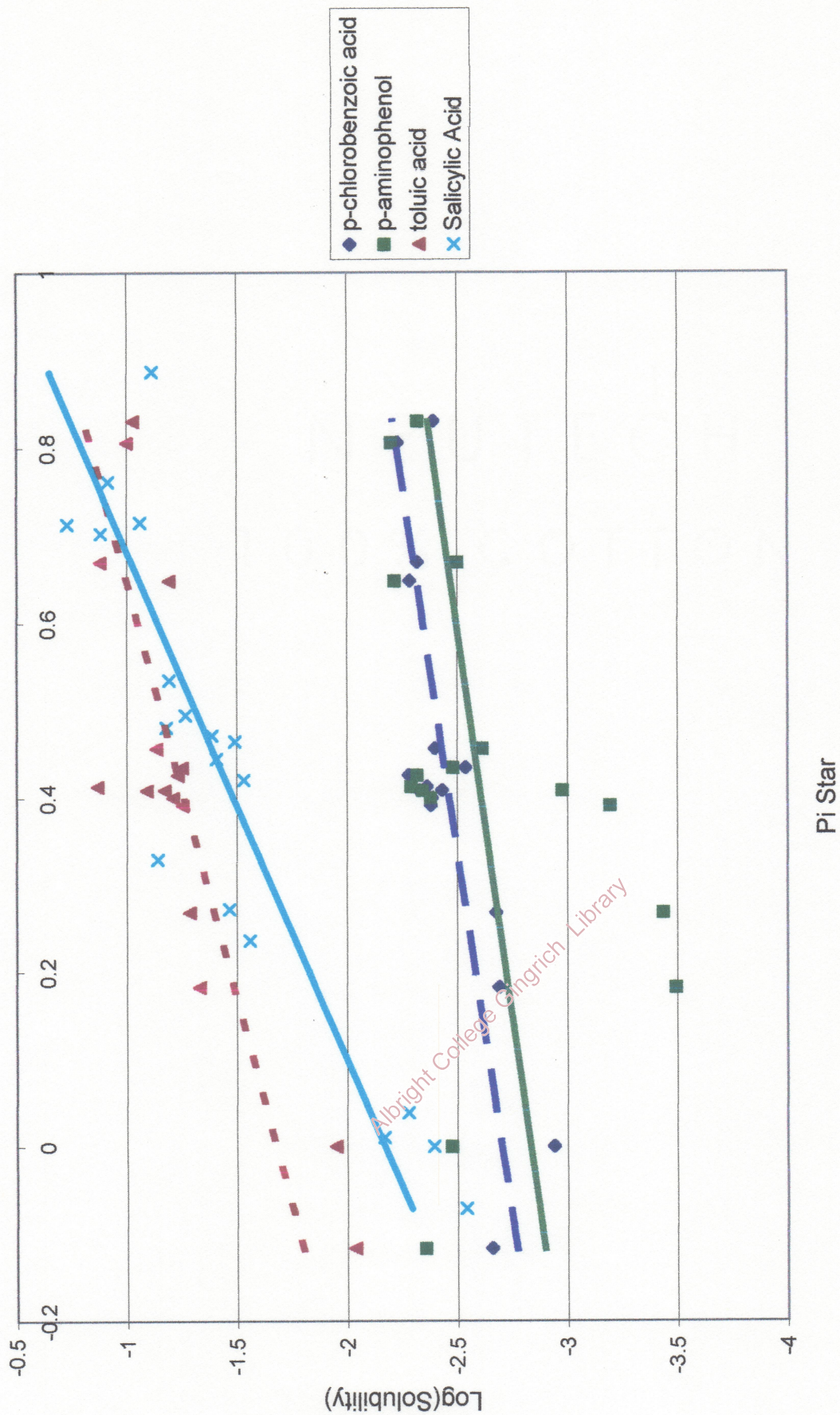


Figure 27: Pi Star vs. Log(Solubility)

